# Crossover phenomena in spin models with medium-range interactions and self-avoiding walks with medium-range jumps

Sergio Caracciolo,[1,*] Maria Serena Causo,[2,†] Andrea Pelissetto,[3,‡] Paolo Rossi,[4,§] and Ettore Vicari[4,‖]

[1]*Scuola Normale Superiore, INFN and INFM, I-56100 Pisa, Italy*
[2]*Scuola Normale Superiore and INFM, I-56100 Pisa, Italy*
[3]*Dipartimento di Fisica, Università di Roma La Sapienza and INFN, Sezione di Roma, I-00185 Roma, Italy*
[4]*Dipartimento di Fisica, Università di Pisa and INFN, Sezione di Pisa, I-56100 Pisa, Italy*

We study crossover phenomena in a model of self-avoiding walks with medium-range jumps, which corresponds to the limit $N \to 0$ of an $N$-vector spin system with medium-range interactions. In particular, we consider the critical crossover limit that interpolates between the Gaussian and the Wilson-Fisher fixed point. The corresponding crossover functions are computed by using field-theoretical methods and an appropriate mean-field expansion. The critical crossover limit is accurately studied by numerical Monte Carlo simulations, which are much more efficient for walk models than for spin systems. Monte Carlo data are compared with the field-theoretical predictions for the critical crossover functions, finding good agreement. We also verify the predictions for the scaling behavior of the leading nonuniversal corrections. We determine phenomenological parametrizations that are exact in the critical crossover limit, have the correct scaling behavior for the leading correction, and describe the nonuniversal crossover behavior of our data for any finite range.

PACS number(s): 05.70.Jk, 64.60.Fr, 75.10.Hk, 61.25.Hq

## I. INTRODUCTION

The universality of critical phase transitions is related to the presence of a diverging correlation length $\xi$. When $\xi$ is much larger than any microscopic scale characterizing the system, one observes a scaling behavior that is universal, i.e., independent of the microscopic details. However, in experimental situations the correlation length may not be so large and, on the contrary, it may be comparable to some other scale intrinsic to the system. In this case, one does not observe the expected critical behavior, but rather a crossover. Here, we will be interested in the crossover between the standard Wilson-Fisher behavior (near the critical point) and the mean-field behavior (far from the critical point) that is observed by varying the temperature in systems belonging to the $N$-vector universality class, i.e., magnets, fluids, multicomponent fluid mixtures, . . . (the critical behavior of these systems is reviewed, e.g., in Refs. [1,2]). Such a crossover is characterized by the Ginzburg number $G$ [3] that measures the relevance of the magnetization (or density) space fluctuations that determine the departure from the Landau mean-field behavior. If $t \equiv (\beta_c - \beta)/\beta_c$ is the reduced temperature, for $|t| > G$ the system shows an approximate mean-field behavior, while for $|t| < G$ one observes the standard Wilson-Fisher criticality. The crossover behavior is nonuniversal since it depends on the specific details of the system under investigation, and is usually described in terms of phenomenological models (see, e.g., Refs. [4–18] and reference therein for a discussion of phenomenological models for flu-

ids, binary mixtures, and polymers). However, in a specific limit—we call it the critical crossover limit—one can define universal quantities that do not depend on the microscopic details.

In this paper, we will consider spin models with medium-range interactions. For instance, we may consider the Hamiltonian

$$H = -\sum_x \sum_{y:|y-x| \leqslant R} \sigma_x \sigma_y, \qquad (1)$$

where $\sigma_x$ is an $N$-component vector satisfying $\sigma_x \sigma_x = 1$. The crossover behavior of these systems has been extensively studied numerically [19–24,15]. By means of scaling arguments, it was shown [19–21] that the Ginzburg number $G$ is proportional to $R^{-2d/(4-d)}$ in $d$ dimensions. Thus, for $|t| \gg R^{-2d/(4-d)}$, such systems show an approximate mean-field behavior, while for $|t| \ll R^{-2d/(4-d)}$, one observes the standard Wilson-Fisher criticality.

Such a crossover can be described by using effective exponents. For instance, one can define an effective susceptibility exponent $\gamma_{\text{eff}}(t)$ (often called the Kouvel-Fisher exponent [25]) by

$$\gamma_{\text{eff}}(t,R) = -\frac{t}{\chi_R(t)} \frac{d\chi_R(t)}{dt}, \qquad (2)$$

where $\chi_R(t)$ is the susceptibility. By varying the temperature, the exponent $\gamma_{\text{eff}}(t,R)$ varies between 1, the mean-field value, and $\gamma$, the Wilson-Fisher value (actually, the full crossover behavior can be observed only for $R$ large enough, in lattice models for $R \gtrsim 3$). At $R$ fixed, the crossover behavior is not universal, and therefore the function $\gamma_{\text{eff}}(t,R)$ at fixed $R$ cannot be predicted without an explicit reference to the microscopic details of the system. In this case, if one wishes to obtain interpolations that provide reasonably pre-

*Email address: Sergio.Caracciolo@sns.it
†Email address: causo@cibs.sns.it
‡Email address: Andrea.Pelissetto@roma1.infn.it
§Email address: Paolo.Rossi@df.unipi.it
‖Email address: Ettore.Vicari@df.unipi.it

cise approximations, one must resort to phenomenological models, such as those presented in Refs. [4–17]. However, there is a particular limit—the critical crossover limit—in which the effective exponents become universal. If we consider the limit $t \to 0, R \to \infty$ with $\tilde{t} \equiv t/G \sim tR^{2d/(4-d)}$ fixed, then $\gamma_{\text{eff}}(t,R)$ converges to a critical crossover exponent $\gamma_{\text{eff}}(\tilde{t})$ that is universal apart from a trivial rescaling of $\tilde{t}$. In practice, at least in lattice models such as Eq. (1), the critical crossover functions provide a good description of the crossover as soon as the interactions extend over a few (two or three) lattice spacings.

The universality of the critical crossover functions can be shown explicitly in the large-$N$ limit [26,27] and for any value of $N$ by performing an expansion around mean field [27]. Moreover, as shown in Ref. [27], they are given *exactly* by the field-theoretical crossover curves computed within the $\phi^4$ framework in Refs. [28–32].

In this paper, we wish to check with a high-precision simulation the field-theoretical predictions of Ref. [27]. Large-scale Monte Carlo results have already been obtained for the Ising model, both in two and in three dimensions [20–23]. However, because of the difficulty of keeping under control the finite-size effects, only small ranges $R$ were simulated near the Wilson-Fisher point. Although the general trend of the data was consistent with the analytic field-theoretical predictions, in the Wilson-Fisher region a high-precision numerical test has not yet been done. The considered values of $R$ were too small and there were significant discrepancies between numerical data and theoretical predictions.

Here, we address the problem for a spin model in the limit $N \to 0$, which can be described in terms of self-avoiding walks (SAW's) [33–38]. The advantage of such a system is that we can now work directly in the infinite-volume limit without finite-size effects and thus we can investigate systems with much larger values of the correlation length (in this paper we reach $\xi \approx 500$ for systems in which the interaction extends up to 12 lattice spacings). In the limit $N \to 0$, the model (1) is mapped into a model of SAW's with medium-range jumps, i.e., of SAW's such that the length of each link is less than or equal to $R$. As usual in walk simulations, we work in a monodisperse ensemble, i.e., with walks of fixed length $n$. The length $n$ replaces here the reduced temperature $t$. Medium-range SAW's show a crossover behavior depending on $nG \sim nR^{-2d/(4-d)}$. For $n \ll R^{2d/(4-d)}$, the SAW behaves as an ordinary random walk (mean-field behavior), while in the opposite regime the self-repulsion becomes important and one observes the standard critical behavior. As we already stressed, for fixed values of $R$, such a behavior is not universal and can only be described phenomenologically. There is, however, a universal limit, the *critical* crossover limit: If we take the limit $n \to \infty, R \to \infty$ keeping $\tilde{n} = nR^{-2d/(4-d)}$ fixed, the crossover functions become universal, and can again be computed by using field-theory methods.

The paper is organized as follows. In Sec. II, we introduce the model and the basic observables we consider. In Sec. III, we discuss the critical crossover limit. In Sec. III A, we de-

fine the limit in spin models [20–22] and review the results of Ref. [27]. In Sec. III B, we define the crossover limit for walk models and derive some general results for the universal crossover functions. In particular, we show that they are *exactly* related to the crossover functions computed in field theory [39–41]. Moreover, by using the results of Ref. [27], we show that by an appropriate definition of the range $R$, the leading corrections to the universal crossover functions scale as $R^{-d}$, $d$ being the dimension, as $R \to \infty$. In Sec. IV, we derive the expressions of the crossover functions from field theory generalizing the results of Ref. [40]. Details are reported in the Appendix, where we also compute the first coefficients of the asymptotic expansion of the crossover functions near the Wilson-Fisher point by using the fixed-dimension expansion in the zero-momentum scheme [42] and in the dimensional regularization scheme without $\epsilon$ expansion [43,31,32]. In Sec. V, we briefly describe the numerical algorithms we use. In Sec. VI, we perform a detailed comparison of the numerical results in three dimensions with the field-theory predictions. We find a very good agreement, the deviations being small already when the interaction extends over three lattice spacings. Particular care has been devoted to the behavior of the leading corrections. We show that they scale as $R^{-d}$ as predicted in Ref. [27]. Finally, in Sec. VII we report our conclusions and discuss some further applications of these results. In particular, we give phenomenological expressions that are able to describe the crossover curves even outside the critical limit, for all ranges $R$ we have considered. Preliminary results appeared in Ref. [44].

## II. THE MODEL

In this paper, we consider SAW's with medium-range jumps. To be specific, let us consider a hypercubic lattice in $d$ dimensions. Given an integer number $\rho$, let us define a lattice domain $D_\rho(x)$. If $x$ is a lattice point, $D_\rho(x)$ is the set of lattice points defined by

$$D_\rho(x) = \left\{ y : \sum_{i=1}^{d} |x_i - y_i| \leq \rho \right\}. \quad (3)$$

We indicate with $V_\rho$ the number of points belonging to $D_\rho(x)$ and with $R$ the mean-square size of $D_\rho(x)$. Explicitly, we define

$$V_\rho \equiv \sum_{y \in D_\rho(0)} 1, \quad (4)$$

$$R^2 \equiv \frac{1}{2dV_\rho} \sum_{y \in D_\rho(0)} y^2. \quad (5)$$

In three dimensions,

$$V_\rho = \tfrac{1}{3}(2\rho+1)(2\rho^2+2\rho+3), \quad (6)$$

$$R^2 = \frac{\rho(\rho+1)}{10} \frac{\rho^2+\rho+3}{2\rho^2+2\rho+3}. \quad (7)$$

For $\rho \to \infty$, $V_\rho \approx \frac{4}{3}\rho^3$ and $R^2 \approx \frac{1}{20}\rho^2$. In the following, we will often characterize the size of the jumps by using $R$ instead of $\rho$ and thus we will write $D_R, V_R, \ldots$, instead of $D_\rho, V_\rho, \ldots$.

Let us now define our model. We define an $n$-step $R$-SAW as a sequence of lattice points $\{\omega_0, \ldots, \omega_n\}$ with $\omega_0 = (0, \ldots, 0)$ and $\omega_{j+1} \in D_R(\omega_j)$, such that $\omega_i \neq \omega_j$ for all $i \neq j$. All walks are weighted equally. For $\rho = 1$, the model corresponds to a standard SAW with nearest-neighbor jumps.

We will consider the following observables: If $c_{n,R}(x)$ is the number of $n$-step $R$-SAW's going from 0 to $x$, we indicate with $c_{n,R}$ the total number of $n$-step walks and with $E_{n,R}^2$ the mean-square end-to-end distance. They are defined as follows:

$$c_{n,R} \equiv \sum_x c_{n,R}(x), \qquad (8)$$

$$E_{n,R}^2 \equiv \frac{1}{c_{n,R}} \sum_x x^2 c_{n,R}(x). \qquad (9)$$

This model of walks is related to a lattice $N$-vector model with medium-range interactions in the limit $N \to 0$. Indeed, consider the Hamiltonian

$$H_R(\sigma) = -\frac{N}{2} \sum_x \sum_{y \in D_R(x)} \sigma_x \sigma_y, \qquad (10)$$

where $\sigma_x$ is an $N$-dimensional vector satisfying $\sigma_x \sigma_x = 1$, and define as usual

$$Z_R(\beta) \equiv \sum_{\{\sigma\}} e^{-\beta H_R(\sigma)}, \qquad (11)$$

$$G_R(x;\beta) \equiv \langle \sigma_0 \sigma_x \rangle_R = \frac{1}{Z_R(\beta)} \sum_{\{\sigma\}} \sigma_0 \sigma_x e^{-\beta H_R(\sigma)}. \qquad (12)$$

The susceptibility and the (second-moment) correlation length are then defined as

$$\chi_R(\beta) \equiv \sum_x G_R(x;\beta), \qquad (13)$$

$$\xi_R^2(\beta) \equiv \frac{1}{2d\chi_R(\beta)} \sum_x x^2 G_R(x;\beta). \qquad (14)$$

A standard procedure [33–38] allows us to prove that

$$\lim_{N \to 0} \chi_R(\beta) = \sum_{n=0}^{\infty} \beta^n c_{n,R}, \qquad (15)$$

$$\lim_{N \to 0} \xi_R^2(\beta)\chi_R(\beta) = \frac{1}{2d} \sum_{n=0}^{\infty} \beta^n c_{n,R} E_{n,R}^2. \qquad (16)$$

This equivalence will allow us to use the results available for the Hamiltonian (10) that are discussed in detail in Ref. [27].

## III. CRITICAL CROSSOVER LIMIT

In this section, we derive some general results for the critical crossover limit of medium-range SAW's. They will be obtained by extending to walk models the results of Ref. [27].

### A. The variable-length $\beta$ ensemble

Let us consider the Hamiltonian (10), which, for $R$ fixed, defines a generalized $N$-vector model with short-range interactions. For each value of $R$, there is a critical point [45] $\beta_{c,R}$; for $\beta \to \beta_{c,R}$, the susceptibility and the correlation length have the standard behavior

$$\chi_R(\beta) \approx A_\chi(R) t^{-\gamma} [1 + B_\chi(R) t^\Delta + \cdots], \qquad (17)$$

$$\xi_R^2(\beta) \approx A_\xi(R) t^{-2\nu} [1 + B_\xi(R) t^\Delta + \cdots], \qquad (18)$$

where $t \equiv (\beta_{c,R} - \beta)/\beta_{c,R}$ and we have neglected additional subleading corrections. The exponents $\gamma$, $\nu$, and $\Delta$ do not depend on $R$. In two dimensions, for $N = 0$, $\gamma$ and $\nu$ are known exactly [46],

$$\nu = \tfrac{3}{4}, \qquad \gamma = \tfrac{43}{32}, \qquad (19)$$

while $\Delta$ is still the object of an intense debate [47–52]. In three dimensions, for $N = 0$, the best estimates of the exponents have been obtained in Monte Carlo simulations:

$$\nu = \begin{cases} 0.5877 \pm 0.0006, & \text{Ref. [53]} \\ 0.58758 \pm 0.00007, & \text{Ref. [54],} \end{cases}$$

$$\gamma = 1.1575 \pm 0.0006, \quad \text{Ref. [55]} \qquad (20)$$

$$\Delta = 0.515^{+0.017}_{-0.007} \quad \text{Ref. [54].}$$

Less precise Monte Carlo results can be found in Refs. [56–59] and references therein. Similar, although less precise, results are obtained by using field-theory methods and from the analysis of enumeration series (for a list of results, see Refs. [40,60–65] and references therein).

On the other hand, the amplitudes are nonuniversal and depend on $R$. For $R \to \infty$, they behave as [20,21]

$$A_\chi(R) \approx A_\chi^\infty R^{2d(1-\gamma)/(4-d)}, \quad A_\xi(R) \approx A_\xi^\infty R^{4(2-d\nu)/(4-d)},$$
$$B_\chi(R) \approx B_\chi^\infty R^{2d\Delta/(4-d)}, \quad B_\xi(R) \approx B_\xi^\infty R^{2d\Delta/(4-d)}. \qquad (21)$$

Corrections to these asymptotic behaviors vanish as [27] $R^{-d}$.

The critical point $\beta_{c,R}$ also depends on $R$. The expansion of $\beta_{c,R}$ for $R \to \infty$ was derived in Ref. [27] in two and three dimensions. Explicitly, for $N = 0$ and $d = 3$, we have

$$\beta_{c,R} = \frac{1}{V_R}\left(1 + \bar{I}_R - \frac{3}{32\pi^2 R^6}\ln R^2 + \frac{\tau_1}{R^6} + \frac{\tau_2}{R^8}\right.$$

$$\left. + O(R^{-9}\ln R^2)\right), \qquad (22)$$

TABLE I. Estimates of $R^3 \bar{I}_R$ for several values of $\rho$ for the domain (3). From Ref. [27].

| $\rho$ | $R^3 \bar{I}_R$ | $\rho$ | $R^3 \bar{I}_R$ |
|---|---|---|---|
| 3 | 0.043960387 | 10 | 0.043486698 |
| 4 | 0.043921767 | 12 | 0.043451767 |
| 5 | 0.043713672 | 14 | 0.043429899 |
| 6 | 0.043664053 | 16 | 0.043415345 |
| 7 | 0.043574469 | 18 | 0.043405187 |
| 8 | 0.043547206 | 20 | 0.043397824 |

where $\tau_1$ and $\tau_2$ are constants and $\bar{I}_R$ is a function of $R$. The nonperturbative constants $\tau_1$ and $\tau_2$ depend on the domain. The expression of $\tau_1$ for a generic domain is reported in Ref. [27]. For the domain (3), $\tau_1 \approx -0.00060(11)$. The constant $\tau_2$ will be computed numerically in Sec. VI A. The function $\bar{I}_R$ is defined by

$$\bar{I}_R \equiv \int \frac{d^3 k}{(2\pi)^3} \frac{1 - \Pi_R(k)}{\Pi_R(k)}, \qquad (23)$$

where

$$\Pi_R(k) \equiv 1 - \frac{1}{V_R} \sum_{x \in D_R(0)} e^{ikx}. \qquad (24)$$

For $R \to \infty$, $\bar{I}_R \approx \sigma R^{-3} + O(R^{-5})$. For the domain considered in this paper, $\sigma \approx 0.04336529$. Explicit values of $\bar{I}_R$ are reported in Table I.

Let us now define the critical crossover limit. In this case, we consider the limit $R \to \infty$, $t \to 0$, with $\tilde{t} \equiv R^{2d/(4-d)} t$ fixed. It is possible to show that

$$\tilde{\chi}_R \equiv R^{-2d/(4-d)} \chi_R(\beta) \to f_\chi(\tilde{t}), \qquad (25)$$

$$\tilde{\xi}_R^2 \equiv R^{-8/(4-d)} \xi_R^2(\beta) \to f_\xi(\tilde{t}), \qquad (26)$$

where the functions $f_\chi(\tilde{t})$ and $f_\xi(\tilde{t})$ are universal apart from an overall rescaling of $\tilde{t}$ and a constant factor. Equations (25) and (26) were predicted in Refs. [20,21] by means of a scaling argument and were proved to all orders in an expansion around $\tilde{t} = \infty$ in Ref. [27].

The crossover functions have a well-defined behavior in the limiting cases $\tilde{t} \to 0$ and $\tilde{t} \to \infty$. For $\tilde{t} \to 0$, Eqs. (17) and (18) imply

$$f_\chi(\tilde{t}) \approx A_\chi^\infty \tilde{t}^{-\gamma} (1 + B_\chi^\infty \tilde{t}^\Delta + \cdots), \qquad (27)$$

$$f_\xi(\tilde{t}) \approx A_\xi^\infty \tilde{t}^{-2\nu} (1 + B_\xi^\infty \tilde{t}^\Delta + \cdots). \qquad (28)$$

In the limit $\tilde{t} \to \infty$, for generic values of $d$, the crossover functions behave as

$$f_\chi(\tilde{t}) \approx \frac{a_\chi}{\tilde{t}} [1 + \alpha_\chi \tilde{t}^{-\Delta_{\mathrm{mf}}} + O(\tilde{t}^{-2\Delta_{\mathrm{mf}}})], \qquad (29)$$

$$f_\xi(\tilde{t}) \approx \frac{a_\xi}{\tilde{t}} [1 + \alpha_\xi \tilde{t}^{-\Delta_{\mathrm{mf}}} + O(\tilde{t}^{-2\Delta_{\mathrm{mf}}})], \qquad (30)$$

where $\Delta_{\mathrm{mf}} = (4 - d)/2$. It is important to notice that this expansion is corrected by logarithms whenever $d = 4 - 2/k$, $k$ integer, and therefore in the interesting cases $d = 2,3$. For $d = 3$, the neglected terms in Eqs. (29) and (30) are of order $O(\tilde{t}^{-1} \ln \tilde{t})$ and not simply of order $O(\tilde{t}^{-1})$. A detailed derivation of these expansions and of the expressions (29) and (30) is given in Ref. [27] for a much more general model than the one considered here. The constants $a_\chi$, $a_\xi$, $\alpha_\chi$, and $\alpha_\xi$ are given, for $2 < d < 4$, by

$$a_\chi = a_\xi = 1,$$
$$\alpha_\chi = \alpha_\xi = -(4\pi)^{-d/2} \Gamma(1 - d/2). \qquad (31)$$

Additional terms can be computed exactly by using the field-theoretical results of Refs. [28,29], the perturbative series of Refs. [66,60], and the mean-field results of Ref. [27], see Sec. IV.

It is also possible to compute the corrections to Eqs. (25) and (26). On the basis of a two-loop calculation, Ref. [27] conjectured that, if the range is expressed in terms of the variable $R$ defined in Eq. (5) [67], then the corrections [68] scale as $R^{-d}$. Explicitly, in the critical crossover limit we expect

$$\tilde{\chi}_R \to f_\chi(\tilde{t}) + \frac{1}{R^d} h_\chi(\tilde{t}) + \cdots, \qquad (32)$$

$$\tilde{\xi}_R \to f_\xi(\tilde{t}) + \frac{1}{R^d} h_\xi(\tilde{t}) + \cdots. \qquad (33)$$

For $\tilde{t} \to 0$ and $\tilde{t} \to \infty$, the functions $h_\chi(\tilde{t})$ and $h_\xi(\tilde{t})$ have an asymptotic behavior that is analogous to that of the universal crossover functions $f_\chi(\tilde{t})$ and $f_\xi(\tilde{t})$. In Ref. [27], the leading term for $\tilde{t} \to \infty$ was computed, obtaining

$$h_\chi(\tilde{t}) \approx -\frac{E_d}{\tilde{t}}, \quad h_\xi(\tilde{t}) \approx -\frac{E_d}{\tilde{t}}, \qquad (34)$$

where $E_d$ is a domain-dependent constant (see Ref. [27] for its definition). For $d = 3$ and for the domain (3), we have $E_3 \approx 0.058545$.

**B. The fixed-length ensemble**

Given the previous results, it is now a completely standard procedure [38] to obtain the behavior of $c_{n,R}$ and $E_{n,R}^2$. For $n \to \infty$ at $R$ fixed, we obtain the standard behavior

$$c_{n,R} \approx C_\chi(R) \beta_{c,R}^{-n} n^{\gamma-1} [1 + D_\chi(R) n^{-\Delta} + \cdots], \qquad (35)$$

$$E_{n,R}^2 \approx C_E(R) n^{2\nu} [1 + D_E(R) n^{-\Delta} + \cdots], \qquad (36)$$

where

$$C_\chi(R) = \frac{A_\chi(R)}{\Gamma(\gamma)},$$

$$C_E(R) = \frac{2dA_\xi(R)\Gamma(\gamma)}{\Gamma(\gamma+2\nu)},$$

$$D_\chi(R) = \frac{B_\chi(R)\Gamma(\gamma)}{\Gamma(\gamma-\Delta)}, \tag{37}$$

$$D_E(R) = \frac{[B_\chi(R) + B_\xi(R)]\Gamma(\gamma+2\nu)}{\Gamma(\gamma+2\nu-\Delta)} - \frac{B_\chi(R)\Gamma(\gamma)}{\Gamma(\gamma-\Delta)}.$$

For $R \to \infty$, using Eq. (21), we obtain $C_\chi(R) \to C_\chi^\infty R^{2d(1-\gamma)/(4-d)}$, where $C_\chi^\infty = A_\chi^\infty/\Gamma(\gamma)$, with corrections of relative order $R^{-d}$. Similar relations hold for the other amplitudes.

The critical crossover limit is trivially defined by remembering that $n$ is the dual variable (in the sense of Laplace transforms) of $t$. Therefore, we should study the limit $n \to \infty, R \to \infty$ with $\tilde{n} \equiv nR^{-2d/(4-d)}$ fixed. From Eqs. (25) and (26), we obtain that the following limits exist:

$$\tilde{c}_{n,R} \equiv c_{n,R}\beta_{c,R}^n \to g_c(\tilde{n}), \tag{38}$$

$$\tilde{E}_{n,R}^2 \equiv E_{n,R}^2 R^{-8/(4-d)} \to g_E(\tilde{n}), \tag{39}$$

where the functions $g_c(\tilde{n})$ and $g_E(\tilde{n})$ are related by a Laplace transform to $f_\chi(\tilde{t})$ and $f_\xi(\tilde{t})$. Explicitly,

$$f_\chi(t) = \int_0^\infty du\, g_c(u)e^{-ut}, \tag{40}$$

$$f_\xi(t)f_\chi(t) = \frac{1}{2d} \int_0^\infty du\, g_c(u)g_E(u)e^{-ut}. \tag{41}$$

Notice that, while the knowledge of $\beta_{c,R}$ is not required for the definition of $g_E(\tilde{n})$, the critical point is needed to compute $g_c(\tilde{n})$.

The standard critical behavior is obtained for $\tilde{n} \to \infty$. In this limit, we have

$$g_c(\tilde{n}) \approx C_\chi^\infty \tilde{n}^{\gamma-1}(1 + D_\chi^\infty \tilde{n}^{-\Delta} + \cdots), \tag{42}$$

$$g_E(\tilde{n}) \approx C_E^\infty \tilde{n}^{2\nu}(1 + D_E^\infty \tilde{n}^{-\Delta} + \cdots). \tag{43}$$

The mean-field limit corresponds to $\tilde{n} \to 0$. Using Eqs. (29) and (30), we obtain

$$g_c(\tilde{n}) \approx 1 + \zeta_c \tilde{n}^{\Delta_{\text{mf}}} + \cdots, \tag{44}$$

$$g_E(\tilde{n}) \approx 2d\tilde{n}(1 + \zeta_E \tilde{n}^{\Delta_{\text{mf}}} + \cdots), \tag{45}$$

with corrections of order $\tilde{n}^{2\Delta_{mf}}$. In two and three dimensions, additional logarithms appear. For $d=3$, the neglected corrections to $g_c(\tilde{n})$ in Eq. (44) are of order $\tilde{n} \ln \tilde{n}$. However, it can be shown by using the field-theoretical results of Appendix A 3 that the logarithmic terms exponentiate and that one can write

$$g_c(\tilde{n}) = e^{\zeta_{\ln}\tilde{n} \ln \tilde{n}}g_{c\,\ln}(\tilde{n}), \tag{46}$$

where $\zeta_{\ln}$ is a constant and $g_{c,\ln}(\tilde{n})$ is a function with a regular expansion in powers of $\tilde{n}^{\Delta_{\text{mf}}}$ without logarithms. The behavior of $g_E(\tilde{n})$ is simpler: It has a regular expansion in powers of $\tilde{n}^{\Delta_{\text{mf}}}$ in all dimensions without logarithms [39]. The constants $\zeta_c$ and $\zeta_E$ can be easily related to $\alpha_\chi$ and $\alpha_\xi$ defined in Eqs. (29) and (30):

$$\zeta_c = \frac{\alpha_\chi}{\Gamma(1+\Delta_{\text{mf}})}, \tag{47}$$

$$\zeta_E = \frac{\alpha_\chi + \alpha_\xi}{\Gamma(2+\Delta_{\text{mf}})} - \frac{\alpha_\chi}{\Gamma(1+\Delta_{\text{mf}})}. \tag{48}$$

Using the explicit results (31), we obtain in three dimensions

$$\zeta_c = \frac{1}{2\pi^{3/2}}, \quad \zeta_E = \frac{1}{6\pi^{3/2}}. \tag{49}$$

We wish now to compute the corrections to the universal crossover functions. For $R \to \infty$, in the variable-length ensemble, the corrections are $O(R^{-d})$, see Eqs. (32) and (33), for $2 < d < 4$. Thus, we expect that the universal crossover functions in the fixed-length ensemble have the same behavior. Therefore, we write

$$\tilde{c}_{n,R} \to g_c(\tilde{n}) + \frac{1}{R^d}k_c(\tilde{n}), \tag{50}$$

$$\tilde{E}_{n,R}^2 \to g_E(\tilde{n}) + \frac{1}{R^d}k_E(\tilde{n}). \tag{51}$$

It is easy to verify by using the Euler-MacLaurin formula that

$$h_\chi(t) = \int_0^\infty du\, k_c(u)e^{-ut}, \tag{52}$$

$$f_\xi(t)h_\chi(t) + f_\chi(t)h_\xi(t) = \frac{1}{2d}\int_0^\infty du[g_E(u)k_c(u)$$
$$+ g_c(u)k_E(u)]e^{-ut}. \tag{53}$$

The asymptotic behavior of the correction functions $k_c(\tilde{n})$ and $k_E(\tilde{n})$ for $\tilde{n} \to 0$ and $\tilde{n} \to \infty$ is analogous to that of $g_c(\tilde{n})$ and $g_E(\tilde{n})$. For $\tilde{n} \to 0$, by using Eqs. (34), (29), and (30), we obtain

$$k_c(0) = -E_d, \quad k_E(\tilde{n}) = -2dE_d\tilde{n} + O(\tilde{n}^{1+\Delta_{\text{mf}}}). \tag{54}$$

## IV. FIELD-THEORY RESULTS IN THREE DIMENSIONS

We wish now to compute the crossover functions by using field-theory methods. Consider the continuum $\phi^4$ theory,

$$H = \int d^3x\left[\frac{1}{2}(\partial_\mu \phi)^2 + \frac{r}{2}\phi^2 + \frac{u}{4!}\phi^4\right], \tag{55}$$

where $\phi$ is an $N$-dimensional vector—in our case $N=0$—and introduce the Ginzburg number $G\equiv u^{2/(4-d)}$ and $t\equiv r-r_c$, where $r_c$ is the critical value of $r$. Then, consider the limit $u\to0, t\to0$, with $\tilde{t}_{SR}\equiv t/G=tu^{-2/(4-d)}$ fixed. In this limit we have

$$\tilde{\chi}\equiv\chi G\to F_\chi(\tilde{t}_{SR}),\qquad(56)$$

$$\tilde{\xi}^2\equiv\xi^2 G\to F_\xi(\tilde{t}_{SR}).\qquad(57)$$

The functions $F_\chi(\tilde{t}_{SR})$ and $F_\xi(\tilde{t}_{SR})$ can be computed by resumming appropriately the perturbative series. There are essentially two different perturbative series one can consider: (a) the fixed-dimension expansion [42,28,29], which is at present the most precise one since seven-loop series are available [66,60]; (b) the so-called dimensional regularization without $\epsilon$ expansion [43,31,32] that uses five-loop $\epsilon$-expansion results [69,70]. In these two schemes, the crossover functions are expressed in terms of various renormalization-group quantities. The explicit expressions are reported in Appendixes A 1 and A 2. For our purposes, the relevant result is that the functions $F_\chi(\tilde{t}_{SR})$ and $F_\xi(\tilde{t}_{SR})$ are related by simple rescalings (SR) to the crossover functions we have defined before [27]. More precisely,

$$f_\chi(\tilde{t})=\mu_\chi F_\chi(s\tilde{t}),\quad f_\xi(\tilde{t})=\mu_\xi F_\xi(s\tilde{t}),\qquad(58)$$

for appropriate constants $\mu_\chi$, $\mu_\xi$, and $s$. These relations are shown rigorously to all orders in the expansion around the mean-field limit in Ref. [27] and provide the link between medium-range crossover functions and field-theoretical expressions. The constants can be easily computed by comparing the behavior for $\tilde{t}\to\infty$. In three dimensions, the functions $F_\chi(\tilde{t}_{SR})$ and $F_\xi(\tilde{t}_{SR})$ behave as (see Appendix A 1 a)

$$F_\chi(\tilde{t})=\frac{1}{\tilde{t}}\left(1+\frac{1}{12\pi}\tilde{t}^{-1/2}+O(\tilde{t}^{-1}\ln\tilde{t})\right),$$

$$F_\xi(\tilde{t})=\frac{1}{\tilde{t}}\left(1+\frac{1}{12\pi}\tilde{t}^{-1/2}+O(\tilde{t}^{-1}\ln\tilde{t})\right).\qquad(59)$$

By comparing these expansions with Eqs. (29) and (30), we obtain

$$s=\mu_\chi=\mu_\xi=\tfrac{1}{9}.\qquad(60)$$

We can now use the explicit results of the Appendix to obtain predictions for the constants $A_\chi^\infty$, $A_\xi^\infty$, $B_\chi^\infty$, and $B_\xi^\infty$ defined in Eqs. (27) and (28). We obtain in the fixed-dimension expansion (see Appendix A 1 b)

$$A_\chi^\infty=\mu_\chi\chi_0 s^{-\gamma}=0.5959\pm0.0041,\qquad(61)$$

$$A_\xi^\infty=\mu_\xi\xi_0^2 s^{-2\nu}=0.5238\pm0.0024,\qquad(62)$$

$$B_\chi^\infty=\chi_1 s^\Delta=2.18\pm0.18,\qquad(63)$$

$$B_\xi^\infty=\xi_1 s^\Delta=2.92\pm0.27.\qquad(64)$$

For the (universal) ratio $B_\chi^\infty/B_\xi^\infty$ we obtain the more precise result

$$\frac{B_\chi^\infty}{B_\xi^\infty}=0.745\pm0.034.\qquad(65)$$

Consistent, although less precise, results can be obtained in the framework of dimensional regularization without $\epsilon$ expansion, see Appendix A 2 b.

In a completely analogous way, we can derive from field theory the crossover functions $g_c(\tilde{n})$ and $g_E(\tilde{n})$. Indeed, we introduce functions $G_c(\tilde{n}_{SR})$ and $G_E(\tilde{n}_{SR})$ in the following way:

$$F_\chi(t)=\int_0^\infty du\, G_c(u)e^{-ut},\qquad(66)$$

$$F_\xi(t)F_\chi(t)=\frac{1}{2d}\int_0^\infty du\, G_c(u)G_E(u)e^{-ut}.\qquad(67)$$

The functions $G_c(\tilde{n}_{SR})$ and $G_E(\tilde{n}_{SR})$ can be computed perturbatively by using the corresponding perturbative expressions for $F_\chi(\tilde{t}_{SR})$ and $F_\xi(\tilde{t}_{SR})$. The relevant formulas are reported in Appendix A 3.

In the fixed-dimension expansion, using the seven-loop results of Ref. [60], we obtain [the six-loop result for $G_E(\tilde{n}_{SR})$ already appears in Ref. [40]]

$$G_c(\tilde{n}_{SR})=e^{4\pi z^2\ln(Kz)}[1+4z+2\pi\gamma_E z^2-60.7295z^3$$
$$-96.6721z^4-144.431z^5+2491.95z^6$$
$$-5070.31z^7+O(z^8)],\qquad(68)$$

$$G_E(\tilde{n}_{SR})=6\tilde{n}_{SR}\left[1+\frac{4}{3}z+\left(\frac{28\pi}{27}-\frac{16}{3}\right)z^2+6.29688z^3\right.$$
$$-25.0573z^4+116.135z^5-594.717z^6$$
$$\left.+3273.16z^7+O(z^8)\right],\qquad(69)$$

where $K$ is a nonperturbative constant and

$$z=\frac{1}{24\pi}\left(\frac{\tilde{n}_{SR}}{\pi}\right)^{1/2}.\qquad(70)$$

Explicitly,

$$\ln K=144\pi^2 D_3+\tfrac{1}{2}\ln(16\pi)-\tfrac{34}{9},\qquad(71)$$

where $D_3$ is a nonperturbative constant reported in Appendix A 1 a. Numerically, using the estimate of $D_3$ reported in Appendix A 1 a, we have $K=5.44(5)$.

These perturbative expressions can be resummed by using the fact that the series are Borel summable [71–74]. The technical details are reported in Appendix A 3. The resummation is very precise for $z\lesssim1$, with errors smaller than

0.2%. For larger values of $z$ the resummation errors increase and the numerical integration becomes unstable: In practice we have not been able to compute numerically the crossover functions using Eqs. (A87) and (A89) for $z \gtrsim 5$. However, in this region the crossover functions are already well approximated by the asymptotic expansions (A93) and (A94). The resummed expressions are well fitted by the following simple formulas:

$$G_c(\tilde{n}_{SR}) = (1 + 50.793\,65z + 508.5428z^2 + 5929.475z^3$$
$$+ 10\,937.03z^4)^{0.078\,75}, \tag{72}$$

$$G_E(\tilde{n}_{SR}) = 6\tilde{n}_{SR}(1 + 7.611z + 12.051\,35z^2)^{0.175\,166}. \tag{73}$$

The expression for $G_E(\tilde{n}_{SR})$ was proposed in Ref. [54] and it was obtained from a detailed Monte Carlo study of the Domb-Joyce model [75]. We find that the perturbative results are very well described by these expressions, with discrepancies of less than 0.3% for $z < 2$. For larger values of $z$, the differences are slightly larger, of the order of 1%, which is, in any case, of the same order of the error of our resummed results. Note that the expressions (72) and (73) exactly reproduce the small-$z$ behaviors (68) and (69) up to terms of order $O(z^2)$.

The relation between the field-theory functions and $g_c(\tilde{n})$ and $g_E(\tilde{n})$ is straightforward. From Eqs. (58) and (60), we have

$$g_c(\tilde{n}) = \lambda_c G_c(\rho\tilde{n}), \quad g_E(\tilde{n}) = \lambda_E G_c(\rho\tilde{n}), \tag{74}$$

with

$$\lambda_E = \tfrac{1}{9}, \quad \lambda_c = 1, \quad \rho = 9. \tag{75}$$

Using the results of Appendix A 3, we can easily derive estimates for the constants $C_\chi^\infty$, $C_E^\infty$, $D_\chi^\infty$, and $D_E^\infty$ defined in Eqs. (42) and (43). In the fixed-dimension expansion, we have

$$C_\chi^\infty = 0.640 \pm 0.005, \tag{76}$$

$$C_E^\infty = 2.457 \pm 0.011, \tag{77}$$

$$D_\chi^\infty = 1.45 \pm 0.10, \tag{78}$$

$$D_E^\infty = 5.03 \pm 0.48. \tag{79}$$

If we consider the universal ratio $D_\chi^\infty / D_E^\infty$ we obtain the more precise result

$$\frac{D_\chi^\infty}{D_E^\infty} = 0.288 \pm 0.016. \tag{80}$$

We mention that from the very precise Monte Carlo results of Ref. [54], we would obtain $C_E^\infty \approx 2.450$ and $D_E^\infty \approx 5.57$, in reasonable agreement with our results.

## V. ALGORITHMS

The SAW with nearest-neighbor jumps can be very efficiently simulated by means of nonlocal algorithms [76,77]. None of them can be generalized to the case at hand, and thus we have resorted to the dimerization algorithm (DA) [78,79]. Although the CPU time needed to generate a walk increases more than any power of its length [76], the prefactors are so small that we can reach quite large lengths. It should be noticed that other algorithms could have probably performed better. For instance, we could have used the pruned-enriched Rosenbluth method of Ref. [80].

Before defining the DA, let us introduce the simple-sampling algorithm (SSA). The SSA is the simplest algorithm for the generation of SAW's. It builds a walk recursively. Once an $n$-step $R$-SAW $\{\omega_0, \ldots, \omega_n\}$ is generated, an $(n+1)$-step $R$-SAW is obtained by choosing at random a new point $\omega_{n+1}$ in $D_R(\omega_n) \backslash \{\omega_n\}$. If the new walk is self-avoiding it is kept, otherwise the $n$-step $R$-SAW is discarded and the procedure starts again from scratch generating a new $n$-step $R$-SAW. Since adding one step and checking for self-avoidance requires [81] $O(1)$ operations, the CPU time needed to generate an $n$-step walk is

$$T_{CPU}(n) \approx \frac{\beta_{c,mf}^{-n}}{c_n} \sum_{m=1}^{n} c_m \beta_{c,mf}^m, \tag{81}$$

where $\beta_{c,mf} \equiv 1/(V_R - 1)$. In the limit $n \to \infty$ with $R$ fixed and large, using Eqs. (35) and (22), we obtain

$$T_{CPU}(n) \sim R^{d\gamma} n^{(-\gamma+1)} e^{\alpha n R^{-d}}, \tag{82}$$

where $\alpha$ is defined by $\beta_{c,mf}/\beta_{c,R} \approx 1 - \alpha R^{-d}$. For our model, $\alpha \approx 0.035$. The computer time increases exponentially with $n$ although the factor in the exponential goes to zero as $R^{-d}$.

The SSA is quite efficient in generating short walks. However, far from the Gaussian region it becomes too slow, because of the exponentially increasing time needed to generate a walk. A better algorithm is the DA [78,79]. Numerically, we find DA to perform better than SSA for $n \gtrsim V_R$. The DA is again a recursive algorithm. To generate an $n$-step walk one generates two $n/2$-step walks and concentrates them. If the resulting walk is self-avoiding, it is kept, otherwise the two $n/2$-step walks are discarded and the procedure is repeated again. The algorithm is recursive: in order to generate the walks of length $n/2$, the DA is used again until $n/2 < n_c$. If $n/2 < n_c$, we generated the walks using the SSA. In our implementation we chose $n_c \approx V_R$. The behavior of the DA in the limit $n \to \infty$ at $R$ fixed was studied in Ref. [76]. By using the results of Sec. III, one finds

$$T_{CPU}(n) \sim R^{q_1} n^{q_2} \exp\left[ \frac{(\gamma - 1)}{2 \ln 2} \ln^2(n R^{2d(1-\gamma)/(4-d)}) \right], \tag{83}$$

where $q_1$ and $q_2$ are exponents that depend on the specific model and on the implementation of the algorithm.

Let us now discuss how to estimate $E_{n,R}^2$ and $c_{n,R}$ from the simulation. Estimating $E_{n,R}^2$ is completely straightfor-

TABLE II. Monte Carlo results. Here $\beta_{\mathrm{mf}} = (V^R - 1)^{-1}$.

| $\rho$ | $n$ | $\ln E_n^2$ | $\ln(c_n \beta_{\mathrm{mf}}^{-n})$ | $\rho$ | $n$ | $\ln E_n^2$ | $\ln(c_n \beta_{\mathrm{mf}}^{-n})$ |
|---|---|---|---|---|---|---|---|
| 2 | 20 | 4.094106(9) | $-1.570800(12)$ | | 10240 | 11.8470(11) | $-264.3489(44)$ |
| | 30 | 4.556891(21) | $-2.52151(4)$ | | 15360 | 12.31571(93) | $-396.9388(36)$ |
| | 40 | 4.886886(17) | $-3.48884(3)$ | | 30720 | 13.1234(22) | $-794.8075(75)$ |
| | 80 | 5.68682(3) | $-7.42459(6)$ | 5 | 600 | 8.88068(10) | $-8.81049(25)$ |
| | 160 | 6.49153(6) | $-15.39944(14)$ | | 1040 | 9.484413(43) | $-15.51334(13)$ |
| | 320 | 7.29966(12) | $-31.45439(30)$ | | 1200 | 9.64205(17) | $-17.95699(50)$ |
| | 640 | 8.10973(24) | $-63.67150(64)$ | | 2080 | 10.25375(8) | $-31.42686(26)$ |
| | 1280 | 8.92194(54) | $-128.2124(16)$ | | 2400 | 10.41268(28) | $-36.3313(10)$ |
| 3 | 120 | 6.50585(3) | $-5.20178(6)$ | | 4160 | 11.03218(14) | $-63.3411(6)$ |
| | 160 | 6.82940(15) | $-7.06537(30)$ | | 8320 | 11.81856(25) | $-127.2624(11)$ |
| | 240 | 7.28750(5) | $-10.81482(13)$ | | 16640 | 12.61152(54) | $-255.2014(24)$ |
| | 320 | 7.61466(26) | $-14.58095(62)$ | | 33280 | 13.4103(11) | $-511.1808(48)$ |
| | 480 | 8.07689(10) | $-22.13565(27)$ | | 66560 | 14.2166(31) | $-1023.251(12)$ |
| | 960 | 8.87276(19) | $-44.87624(56)$ | 6 | 500 | 8.93513(4) | $-4.61781(8)$ |
| | 1920 | 9.67317(37) | $-90.4588(12)$ | | 800 | 9.43841(8) | $-7.52107(20)$ |
| | 3840 | 10.47830(81) | $-181.7297(31)$ | | 1000 | 9.67871(6) | $-9.46419(16)$ |
| 4 | 1200 | 9.39403(32) | $-30.4356(12)$ | | 1600 | 10.18886(14) | $-15.31451(40)$ |
| | 1280 | 9.46739(15) | $-32.4988(5)$ | | 2000 | 10.43242(10) | $-19.22308(33)$ |
| | 1920 | 9.92722(12) | $-49.0221(4)$ | | 3200 | 10.94927(23) | $-30.97376(82)$ |
| | 2560 | 10.25489(28) | $-65.5637(10)$ | | 4000 | 11.19612(18) | $-38.81610(66)$ |
| | 3840 | 10.71901(22) | $-98.6670(8)$ | | 8000 | 11.96920(31) | $-78.0846(13)$ |
| | 5120 | 11.04855(54) | $-131.7917(21)$ | | 16000 | 12.75136(54) | $-156.7110(27)$ |
| | 7680 | 11.51585(45) | $-198.0564(17)$ | | 32000 | 13.5400(11) | $-314.0585(56)$ |

ward. To estimate $c_{n,R}$ we have used the acceptance fraction for the elementary moves of the two algorithms. Indeed, given an $n$-step $R$-SAW, the probability of obtaining an $(n+1)$-step walk using the SSA is simply $c_{n+1}\beta_{c,\mathrm{mf}}/c_n$. Thus, if we know in a given SSA simulation the number $N_n$ of generated walks of length $n$, we can estimate $c_n$ using the recursion relation

$$c_n = c_{n-1}\beta_{c,\mathrm{mf}}^{-1} \frac{N_n}{N_{n-1}}, \qquad (84)$$

with the initial condition $c_1 = \beta_{c,\mathrm{mf}}^{-1}$.

Analogously, given two $R$-SAW's of length $n$, the probability that their concatenation is an $R$-SAW is simply $c_{2n}/c_n^2$. Therefore, if we know in a given DA simulation the number $N_n$ of generated walks of length $n$, we can compute $c_n$ using

$$c_n = c_{n/2}^2 \frac{N_n}{N_{n/2}} \qquad (85)$$

for $n \geq n_c$ and then Eq. (84).

Note that in a dimerization simulation in which we generate walks of maximal length $n_{\max}$, we obtain at the same time estimates of the observables also for a set of smaller values of $n$, i.e., for $n = n_{\max}/2, n_{\max}/4, \ldots$ . These results are of course correlated, especially in the mean-field region where the rejection rate at each step is small. However, for

our global observables, the correlation should be small. Analogously, when we use the SSA, we can compute the observables for all values of $n$, although in this case the results are strongly correlated.

## VI. NUMERICAL RESULTS

We have performed an extensive simulation using three-dimensional walks with $n \leq 66\,560$ and $2 \leq \rho \leq 12$. Notice that the values of $\rho$ are particularly large: for $\rho = 12$, in the spin language, each spin interacts with 2624 neighbors. The advantage of working with SAW's is the absence of finite-size effects—we work in the infinite-volume limit—and the possibility of reaching large values of the correlation length [82]. The raw data for the largest values [83] of $n$ and several values of $\rho$ are reported in Tables II and III.

In Sec. VI A, we will determine $\beta_{c,R}$ from our numerical data and we will explicitly check the theoretical predictions for the large-$R$ behavior of $\beta_{c,R}$ of Ref. [27] presented in Sec. III A. In Sec. VI B, we will compute the critical cross-over functions and we will compare them with the field-theoretical results of Sec. IV.

### A. Determination of $\beta_{c,R}$

In order to compute $\beta_{c,R}$ we define

$$\beta_{\mathrm{eff},R}(n) \equiv \left[ \frac{c_{n,R}}{g_{c,\mathrm{th}}(\tilde{n})} \right]^{-1/n}, \qquad (86)$$

TABLE III. Monte Carlo results. Here $\beta_{mf}=(V^R-1)^{-1}$.

| $\rho$ | $n$ | $\ln E_n^2$ | $\ln(c_n\beta_{mf}^{-n})$ |
|---|---|---|---|
| 7 | 100 | 7.500434(17) | −0.543304(13) |
|  | 200 | 8.214646(25) | −1.164668(26) |
|  | 400 | 8.93561(4) | −2.44010(5) |
|  | 800 | 9.66443(6) | −5.03235(11) |
|  | 1600 | 10.40211(9) | −10.26761(23) |
|  | 3200 | 11.14984(16) | −20.79866(51) |
|  | 6400 | 11.90757(25) | −41.9304(10) |
|  | 12800 | 12.67547(43) | −84.2725(21) |
|  | 25600 | 13.45153(68) | −169.0420(42) |
|  | 51200 | 14.2366(14) | −338.6733(87) |
| 8 | 750 | 9.80702(3) | −3.29563(5) |
|  | 1500 | 10.53428(5) | −6.74019(10) |
|  | 3000 | 11.27031(7) | −13.67826(20) |
|  | 6000 | 12.01591(12) | −27.61282(42) |
|  | 12000 | 12.77156(19) | −55.55008(85) |
|  | 24000 | 13.53685(34) | −111.5009(17) |
|  | 48000 | 14.31143(59) | −223.4866(35) |
| 9 | 1040 | 10.34095(12) | −3.35462(21) |
|  | 2080 | 11.06434(17) | −6.8409(4) |
|  | 4160 | 11.79586(27) | −13.8574(9) |
|  | 8320 | 12.5369(4) | −27.9440(18) |
|  | 16640 | 13.2868(6) | −56.1807(36) |
|  | 33280 | 14.0491(10) | −112.7270(71) |
|  | 66560 | 14.8188(20) | −225.901(14) |
| 10 | 1500 | 10.89765(8) | −3.66081(13) |
|  | 2000 | 11.19598(5) | −4.91804(11) |
|  | 3000 | 11.61839(11) | −7.44241(26) |
|  | 4000 | 11.91986(8) | −9.97288(22) |
|  | 6000 | 12.34684(17) | −15.04661(52) |
|  | 8000 | 12.65209(13) | −20.12732(44) |
|  | 16000 | 13.39353(20) | −40.49032(91) |
|  | 32000 | 14.14511(32) | −81.2802(18) |
|  | 64000 | 14.90648(72) | −162.9324(51) |
| 12 | 1500 | 11.21510(8) | −2.19646(10) |
|  | 2000 | 11.50974(10) | −2.95223(16) |
|  | 3000 | 11.92649(14) | −4.47024(21) |
|  | 4000 | 12.22324(16) | −5.9926(4) |
|  | 6000 | 12.64352(20) | −9.0463(4) |
|  | 8000 | 12.94315(25) | −12.1053(8) |
|  | 12000 | 13.36771(30) | −18.2350(9) |
|  | 16000 | 13.67113(37) | −24.3704(16) |
|  | 32000 | 14.40765(57) | −48.9504(31) |

where $g_{c,th}(\tilde{n})$ is the theoretical crossover function: in our numerical determination of $\beta_{eff,R}(n)$ we will use [84] Eqs. (74) and (A106). By using Eqs. (35) and (42), we obtain for $n\to\infty$

$$\beta_{eff,R}(n)=\beta_{c,R}\left[1-\frac{1}{n}\ln\left(\frac{C_\chi(R)R^{6(\gamma-1)}}{C_\chi^\infty}\right)\right.$$

$$\left.+\frac{1}{n^{1+\Delta}}[D_\chi(R)-D_\chi^\infty R^{6\Delta}]+\cdots\right]. \qquad (87)$$

Using the asymptotic expansions (21) and the relations (37), we obtain for $R\to\infty$

$$\beta_{eff,R}(n)=\beta_{c,R}\left[1+\frac{\alpha_1}{nR^3}+\frac{\alpha_2 R^{6\Delta-3}}{n^{1+\Delta}}+\cdots\right], \qquad (88)$$

where $\alpha_1$ and $\alpha_2$ are $R$-independent constants. This expression shows the advantage of the definition (86) over the common one in which one simply considers $(c_{n,R})^{-1/n}$. Indeed, with our choice, the $1/n$ correction vanishes for $R\to\infty$ while the $1/n^{1+\Delta}$ remains approximately constant ($\Delta\approx\frac{1}{2}$); with the other one, we would have corrections of order $\ln(nR^{-6})/n$ and $R^{6\Delta}/n^{1+\Delta}$. This improved behavior is particularly important, since for large $R$ we are quite far from the Wilson-Fisher point, and thus a reduction of the scaling corrections is essential in order to obtain precise estimates of $\beta_{c,R}$. In order to determine $\beta_{c,R}$, we have performed fits of the form [85]

$$\beta_{eff,R}(n)V_R=\beta_{c,R}V_R+\frac{a}{n}+\frac{bR^{6\Delta}}{n^{1+\Delta}}, \qquad (89)$$

assuming $\Delta=\frac{1}{2}$. We have repeated the fit several times, considering each time only the data satisfying $n\geq n_{min}$. The final results, reported in Table IV, correspond to the smallest $n_{min}$ for which $\chi^2/\text{d.o.f.}\approx1$ (d.o.f. is the number of degrees of freedom). Notice that, by rescaling $b$ by $R^3$, the coefficients $a$ and $b$ should become $R$-independent as $R$ increases. This is evident for $a$ and indeed we can roughly estimate $a\approx-0.015(5)$ for $R\to\infty$. This allows us to compute the leading correction to $C_\chi(R)$. We have

$$C_\chi(R)\approx C_\chi^\infty R^{6(1-\gamma)}(1+\kappa_\chi R^{-3}+\cdots), \qquad (90)$$

where $\kappa_\chi=-a$. The results for $b$ are less stable, but still reasonably compatible with a constant for large $R$. In order to understand the systematic errors due to the truncation (89), we have repeated the fit with an additional correction:

$$\beta_{eff,R}(n)V_R=\beta_{c,R}V_R+\frac{a}{n}+\frac{bR^{6\Delta}}{n^{1+\Delta}}+\frac{cR^6}{n^2}. \qquad (91)$$

The results for $\beta_{c,R}$ do not differ significantly from those of the fit with $c=0$, except for $\rho=12$, where the difference is approximately three combined error bars. Therefore, our final estimates should be quite reliable. As an additional check, we have compared our results with the theoretical prediction (22). If we indicate with $\beta_{c,R}^{(exp)}$ the expansion (22) neglecting terms of order $R^{-8}$, we define

$$\tau_{2,eff}\equiv R^8\left(\frac{\beta_{c,R}}{\beta_{c,R}^{(exp)}}-1\right). \qquad (92)$$

If we have correctly determined $\beta_{c,R}$, $\tau_{2,eff}$ should converge to the constant $\tau_2$ as $R\to\infty$, with corrections of order $\log_{10}R^2/R$. The plot of $\tau_{2,eff}$ is reported in Fig. 1. A fit of the form $\tau_{2,eff}=\tau_2+b/R$ gives

TABLE IV. Determination of $\beta_{c,R}$ for several values of $\rho$. The reported results are obtained by fitting the numerical data with $n > n_{\min}$. Fit (a): $V_R\beta_{\text{eff},R}(n) = V_R\beta_{c,R} + a/n + bR^3/n^{1.5}$. Fit (b): $V_R\beta_{\text{eff},R}(n) = V_R\beta_{c,R} + a/n + bR^3/n^{1.5} + cR^6/n^2$.

| $\rho$ | $n_{\min}$ | $V_R\beta_{c,R}$ | $a$ | $b$ | $c$ |
|---|---|---|---|---|---|
| | | | Fit (a) | | |
| 2 | 40 | 1.152388(1) | 0.0725(4) | 0.1044(16) | |
| 3 | 80 | 1.0656569(3) | 0.0142(3) | 0.0360(5) | |
| 4 | 150 | 1.0342660(1) | −0.0040(3) | 0.0174(3) | |
| 5 | 260 | 1.0199238(1) | −0.0111(1) | 0.0100(1) | |
| 6 | 400 | 1.0125749(1) | −0.0138(4) | 0.0066(2) | |
| 7 | 800 | 1.00840580(4) | −0.0164(3) | 0.0053(1) | |
| 8 | 1500 | 1.00588845(3) | −0.0174(4) | 0.0044(1) | |
| 9 | 1040 | 1.00427552(9) | −0.0140(10) | 0.0026(2) | |
| 10 | 3000 | 1.00320022(5) | −0.0167(13) | 0.0031(3) | |
| 12 | 2000 | 1.00192307(7) | −0.0080(11) | 0.0010(1) | |
| | | | Fit (b) | | |
| 2 | 10 | 1.152388(1) | 0.0711(1) | 0.1211(3) | −0.01139(6) |
| 3 | 15 | 1.0656574(3) | 0.0121(1) | 0.0442(1) | −0.00182(1) |
| 4 | 40 | 1.0342661(1) | −0.0057(1) | 0.0217(1) | −0.000589(6) |
| 5 | 70 | 1.0199239(1) | −0.0130(1) | 0.132(1) | −0.000274(3) |
| 6 | 100 | 1.0125750(1) | −0.0158(4) | 0.0090(2) | −0.000152(6) |
| 7 | 140 | 1.00840566(10) | −0.0159(4) | 0.0062(1) | −0.000081(3) |
| 8 | 300 | 1.00588839(5) | −0.0176(5) | 0.0055(2) | −0.000071(3) |
| 9 | 250 | 1.00427551(10) | −0.0153(10) | 0.0037(2) | −0.000037(3) |
| 10 | 450 | 1.00320011(4) | −0.0143(5) | 0.0030(1) | −0.000028(1) |
| 12 | 400 | 1.00192275(6) | −0.0028(5) | 0.0006(1) | −0.000003(1) |

$$\tau_2 = -0.008\,14(21), \tag{93}$$

$b = 0.002\,77(19)$, including all data with $\rho \geq 3$.

**B. Determination of the critical crossover functions**

We wish now to determine the critical crossover functions in three dimensions. We begin by studying the function $\tilde{c}_{n,R}$,
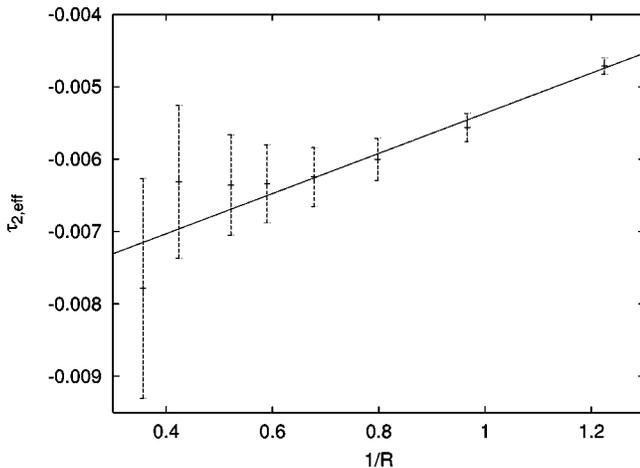


FIG. 1. Estimates of $\tau_{2,\text{eff}}$ vs $1/R$. The reported points correspond to $\rho = 3,4,5,6,7,8,10,12$. The line is the best fit: $\tau_{2,\text{eff}} = -0.00814 + 0.00277/R$. The errors on the data take into account the error on $\beta_{c,R}$ and on the constant $\tau_1$.

cf. Eq. (38). The function is reported in Fig. 2 (upper graph) together with the theoretical prediction obtained by using Eqs. (74) and (72). Note that there is no free parameter in the theoretical curve. We observe a very good agreement, especially in the Wilson-Fisher region. Systematic deviations are observed for smaller values of $\tilde{n}$. In order to understand the role of the deviations, we report in Fig. 2 (lower graph) the same data, but now we exclude all points with $n < V_R/2$. The agreement is now perfect for all $\rho \geq 3$. We thus clearly see that the crossover behavior requires $n \gg R^d$. In particular, mean-field behavior is always observed for $n \ll R^{2d/(4-d)}$ if $R$ is sufficiently large, but it is described by the critical crossover curves only if $R^d \ll n \ll R^{2d/(4-d)}$.

In order to see the corrections to scaling, in Fig. 3 we report the ratio $\tilde{c}_{n,R}/g_{c,\text{th}}(\tilde{n})$, which should converge to 1 as $R \to \infty$. Corrections to scaling are clearly evident, points with different values of $R$ lying on different curves that indeed converge to 1 as $R \to \infty$. These corrections are predicted to scale as $R^{-d}$. To check this behavior, we considered

$$\Delta_{c;n,R} \equiv R^3\left(\frac{\tilde{c}_{n,R}}{g_{c,\text{th}}(\tilde{n})} - 1\right), \tag{94}$$

which should converge to $k_c(\tilde{n})/g_c(\tilde{n})$ in the crossover limit. Using the expected asymptotic behavior of $k_c(\tilde{n})$ and $g_c(\tilde{n})$, $\Delta_{c;n,R}$ converges to a constant both for $\tilde{n} \to 0$ and $\tilde{n} \to \infty$. For $\tilde{n} \to 0$, $k_c(0)/g_c(0) = -E_3 \approx -0.059$.

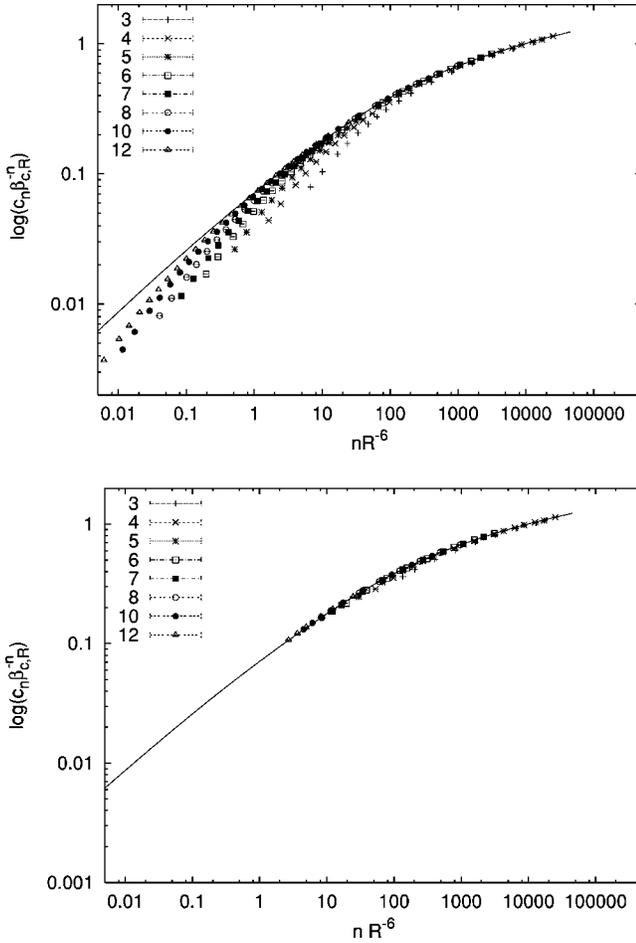The numerical results are reported in Fig. 4, where the

FIG. 2. Estimates of $\log_{10} \widetilde{c}_{n,R}$ vs $\widetilde{n} = nR^{-6}$. The reported points correspond to $\rho = 3,4,5,6,7,8,10,12$. The line is the field-theoretical prediction. In the upper graph we report all points, in the lower one only those satisfying $n > V_R/2$.

error on $\Delta_{c;n,R}$ has been computed by considering the error on $\beta_{c,R}$, $c_{n,R}$, and on the theoretical curve [86]. A reasonably good scaling is observed, confirming the results of Ref. [27]. Also the prediction $k_c(0)/g_c(0) \approx -0.059$ is fully compatible with the data.

In order to perform a more precise check, we have also considered the quantity

$$Q_{n,R} \equiv \frac{c_{n,R}^2}{c_{2n,R}}, \tag{95}$$

that converges to $g_c(\widetilde{n})^2/g_c(2\widetilde{n})$ in the critical crossover limit. For $Q_{n,R}$ we do not need the value of $\beta_{c,R}$ and thus a source of error is avoided. In Fig. 5, we show $Q_{n,R}$ together with the theoretical prediction and

$$\Delta_{Q;n,R} \equiv R^3 \left( \frac{Q_{n,R} g_{c,\text{th}}(2\widetilde{n})}{g_{c,\text{th}}(\widetilde{n})^2} - 1 \right). \tag{96}$$

The errors on $\Delta_{Q;n,R}$ have been computed as we did for $\Delta_{c;n,R}$. The agreement between the numerical data and the
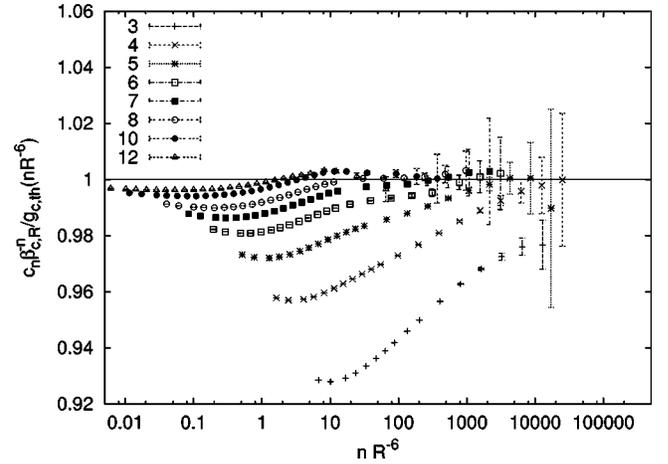


FIG. 3. Estimates of $\widetilde{c}_{n,R}/g_{c,\text{th}}(\widetilde{n})$ vs $\widetilde{n} = nR^{-6}$. The reported points correspond to $\rho = 3,4,5,6,7,8,10,12$. The errors only take into account the error on $\widetilde{c}_{n,R}$.

theoretical prediction is very good. Also, $\Delta_{Q;n,R}$ shows a nice scaling behavior confirming that the corrections scale as $R^{-d}$.

Let us finally discuss the effective exponent $\gamma_{\text{eff}}(n,R)$. A standard definition would be

$$\gamma_{\text{eff}}(n,R) \equiv 1 + n \frac{d \ln \widetilde{c}_{n,R}}{dn}. \tag{97}$$

However, this definition is not easy to use in numerical simulations since it involves the derivative with respect to $n$. Here, we will use the definition

$$\gamma_{\text{eff}}(n,R) \equiv 1 + \frac{1}{\ln 2} \ln \left( \frac{\widetilde{c}_{2n,R}}{\widetilde{c}_{n,R}} \right), \tag{98}$$

which interpolates between the SAW value $\gamma = 1.1575$ and the mean-field value $\gamma = 1$. The results are reported in Fig. 6 together with the theoretical prediction. The agreement is very good. Note that in the Wilson-Fisher region the numerical data are well approximated by the field-theoretical pre-
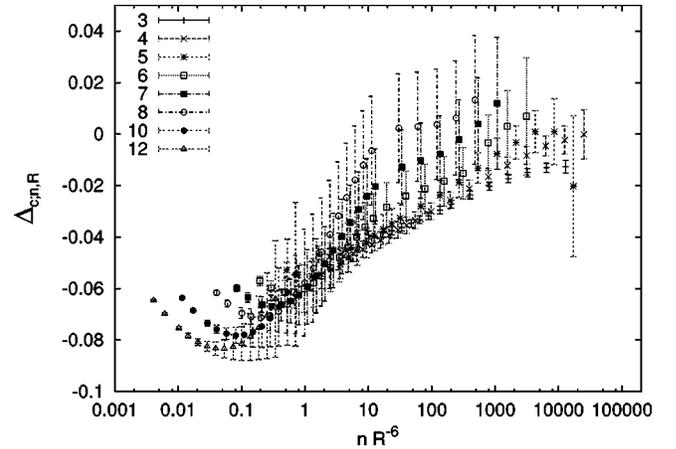


FIG. 4. Estimates of $\Delta_{c;n,R}$ vs $\widetilde{n} = nR^{-6}$. The reported points correspond to $\rho = 3,4,5,6,7,8,10,12$.
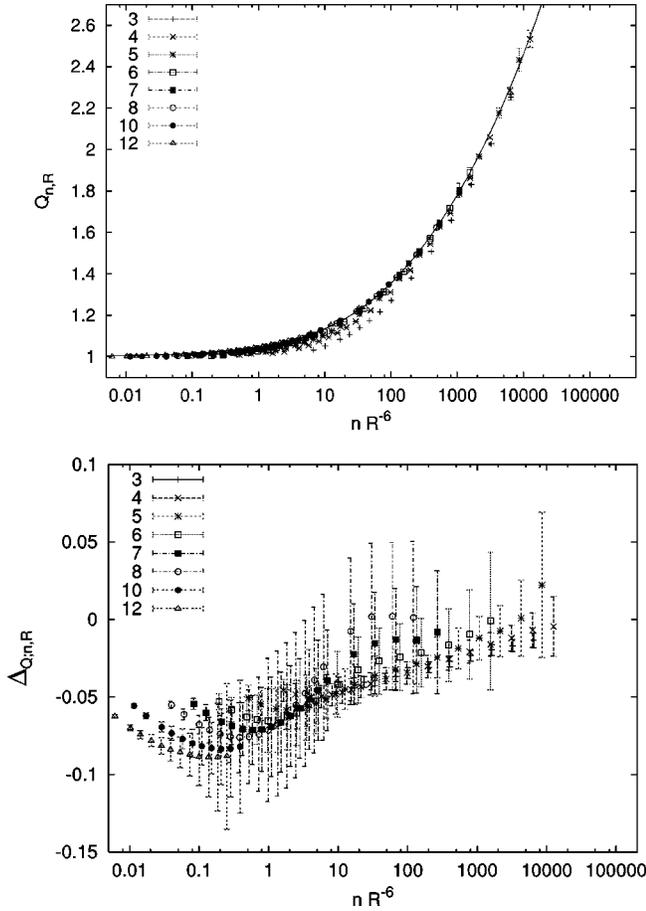
FIG. 5. Estimates of $Q_{n,R}$ (upper graph) and of $\Delta_{Q;n,R}$ (lower graph) vs $\tilde{n} = nR^{-6}$. The reported points correspond to $\rho = 3,4,5,6,7,8,10,12$. The continuous line in the upper graph is the theoretical prediction.
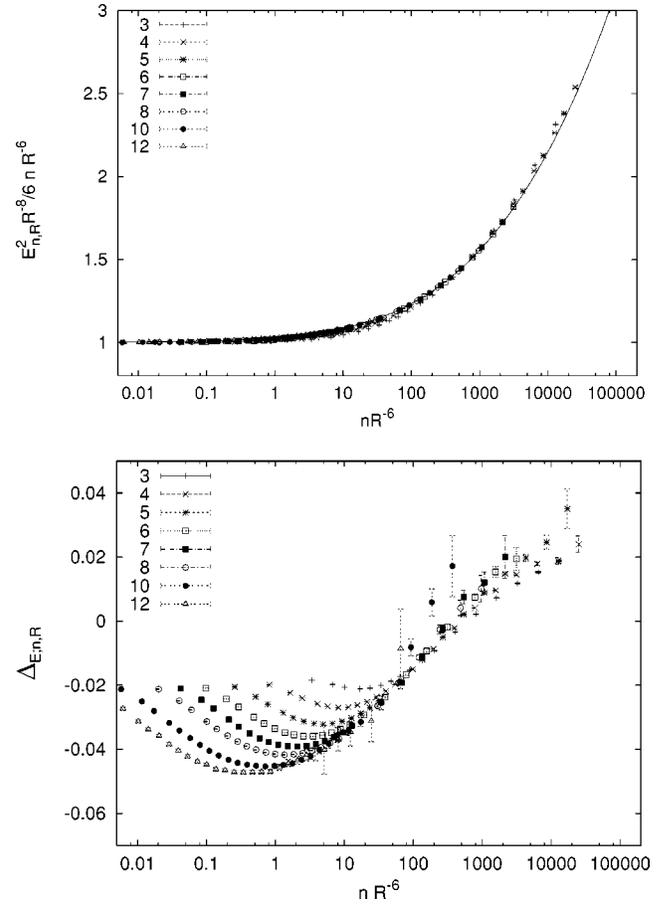


FIG. 7. Estimates of $\tilde{E}^2_{n,R}/(6\tilde{n})$ (upper graph) and of $\Delta_{E;n,R}$ (lower graph) vs $\tilde{n} = nR^{-6}$. The reported points correspond to $\rho = 3,4,5,6,7,8,10,12$. The continuous line in the upper graph is the theoretical prediction.

diction only for $\rho \gtrsim 4$. For smaller values of $\rho$, the corrections are important, as was already noticed in the Ising model simulations [22,23].

The analysis we have performed for $c_{n,R}$ can be repeated



FIG. 6. Estimates of $\gamma_{\text{eff}}(n,R)$ vs $\tilde{n} = nR^{-6}$. The reported points correspond to $\rho = 2,3,4,5,6,7,8,10,12$. The continuous line is the theoretical prediction.

for $E^2_{n,R}$. In this case, however, the errors are smaller since the critical crossover functions do not depend on $\beta_{c,R}$. In Fig. 7 (upper graph), we report our results for $\tilde{E}^2_{n,R}$ together with the prediction $g_{E,\text{th}}(\tilde{n})$ obtained by using the field-theory result (73) and the relations (74) and (75). Note that there is no free parameter in the theoretical curve. The agreement is very good, although one can see clearly the presence of corrections to scaling.

We wish now to compute the correction curve $k_E(\tilde{n})$. For this purpose we consider

$$\Delta_{E;n,R} \equiv R^3 \left( \frac{\tilde{E}^2_{n,R}}{g_{E,\text{th}}(\tilde{n})} - 1 \right), \tag{99}$$

which converges to $k_E(\tilde{n})/g_E(\tilde{n})$ as $R \to \infty$. The plot of $\Delta_{E;n,R}$ is reported in Fig. 7 (lower graph), where we have taken into account only the error on $\tilde{E}^2_{n,R}$. A good scaling behavior is observed confirming the theoretical prediction for the corrections. Moreover, this nice scaling behavior is also an indication that the approximation (73) can be considered at our level of precision practically exact. Note also that the prediction $k_E(0)/g_E(0) = -0.059$, cf. Eq. (54), is in good agreement with our data.
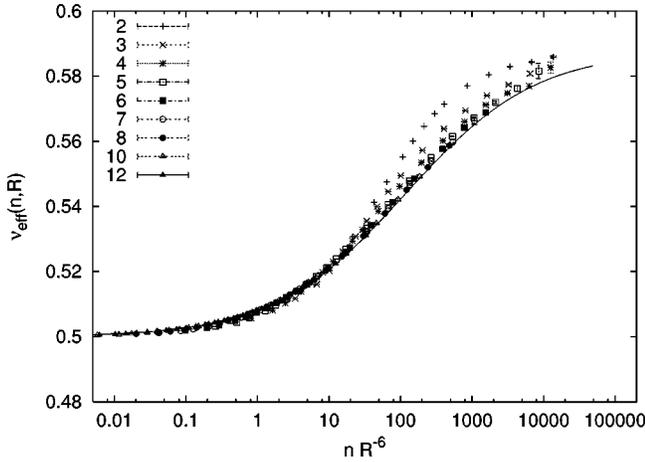
FIG. 8. Estimates of $\nu_{\mathrm{eff}}(n,R)$ vs $\tilde{n}=nR^{-6}$. The reported points correspond to $\rho=2,3,4,5,6,7,8,10,12$. The continuous line is the theoretical prediction.

Let us finally discuss the effective exponent $\nu_{\mathrm{eff}}$. As we did for $\gamma_{\mathrm{eff}}$, instead of

$$\nu_{\mathrm{eff}}(n,R)\equiv n\,\frac{d\ln E_{n,R}^2}{dn}, \qquad (100)$$

we will consider

$$\nu_{\mathrm{eff}}(n,R)\equiv \frac{1}{2\ln 2}\ln_{10}\left(\frac{E_{2n,R}^2}{E_{n,R}^2}\right), \qquad (101)$$

which is easier to compute numerically. A graph of this quantity is reported in Fig. 8. It shows the expected behavior: for $\tilde{n}\to 0$ it converges to $\frac{1}{2}$, while for $\tilde{n}\to\infty$ it converges to $\nu_{\mathrm{SAW}}\approx 0.588$. The agreement with the perturbative prediction is quite good in the random-walk region. On the other hand, as $\tilde{n}$ increases the corrections increase, in agreement with similar results obtained for the Ising model [22,23].

## VII. CONCLUSIONS

In this paper, we have studied the critical crossover limit for a model of walks and we have verified numerically the following statements, predicted by field-theoretical and mean-field methods [27].

(i) The critical crossover functions in medium-range models *coincide* with the field-theoretical crossover curves. The nonuniversal constants can be determined by computing the corrections to the mean-field behavior.

(ii) The asymptotic behavior of $\beta_{c,R}$ for $R\to\infty$ can be computed exactly in lattice models up to corrections of relative order $R^{-8}$ by determining the first corrections to the mean-field limit and exploiting the field-theoretical model.

(iii) The corrections to the critical crossover functions decrease as $R^{-d}$ once $R$ is defined as in Eq. (5).

Our numerical results can also be used to determine phenomenological expressions that describe the data for all values of $R$. Here, different procedures can be used. One can consider the phenomenological model of Ref. [87] (with the modifications discussed in Ref. [27] to make it compatible
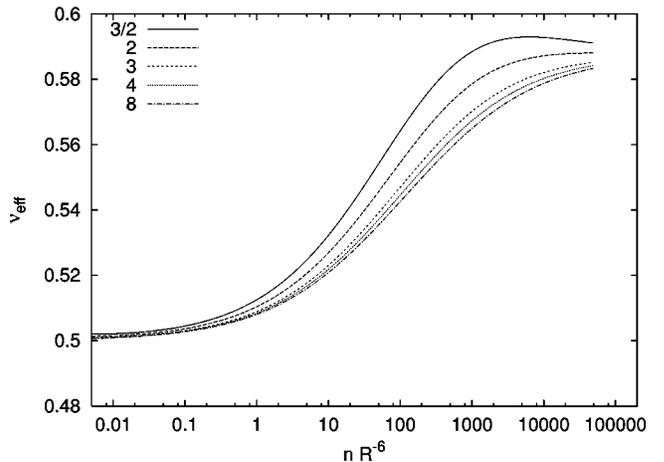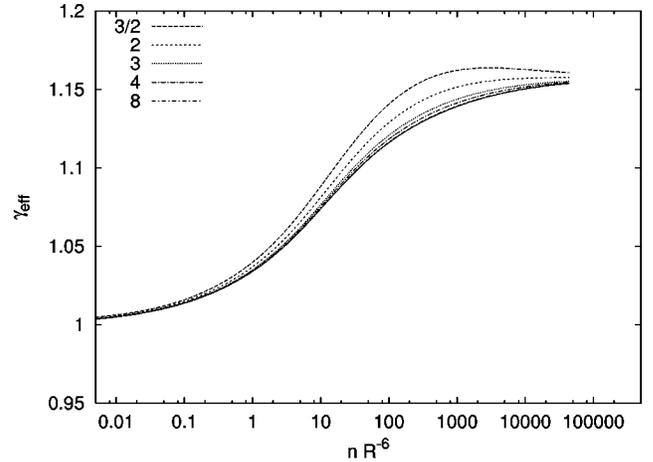




FIG. 9. The effective exponents $\gamma_{\mathrm{eff}}$ (upper curve) and $\nu_{\mathrm{eff}}$ (lower curve) vs $\tilde{n}=nR^{-6}$, obtained from the phenomenological expressions (102) and (103), for several values of $\rho$.

with the theoretical predictions), or the essentially equivalent model discussed in Ref. [9], or one can use the procedure proposed in Ref. [27]. The idea is to write

$$\tilde{c}_{n,R}=g_c(\tilde{n})+R^{-3}k_c(\tilde{n}),$$
$$\tilde{E}_{n,R}^2=g_E(\tilde{n})+R^{-3}k_E(\tilde{n}), \qquad (102)$$

and use a simple parametrization for the correction terms. Here, we approximate

$$k(\tilde{n})=g(\tilde{n})\frac{-0.059+a\tilde{n}^{1/2}+b\tilde{n}}{1+c\tilde{n}^{1/2}+d\tilde{n}} \qquad (103)$$

both for $k_c$ and $k_E$, where we have used the asymptotic behavior (54). The parameters $a$, $b$, $c$, and $d$ are determined by fitting the numerical data. The best results are obtained for $a=-61$, $b=-1.06$, $c=1830$, $d=87$ (function $k_c$) and $a=-23$, $b=0.8505$, $c=972$, $d=32$ (function $k_E$). These fitting functions provide phenomenological expressions that correctly describe our data for all values of $\rho$. The corresponding effective exponents are reported in Fig. 9 and show the typical behavior that has been found in simulations of the Ising model. We have also included in the figure the curves

corresponding to $\rho = \frac{3}{2}$, to show that for $\rho$ small the phenomenological expressions show a nonmonotonic behavior that is not present in the critical crossover curve.

We mention a different approach to the crossover discussed by Nickel [88,54], in which the crossover curves are expressed in terms of a quantity that has a universal critical limit: For polymers the interpenetration ratio is considered, while for spin systems the four-point renormalized coupling would be the variable of choice. This method has the advantage of providing a better description of the nonuniversal deviations in the Wilson-Fisher region.

Although our main motivation was the understanding of spin models, the results of this paper are also relevant in the context of polymers. Indeed, as is well known [37,38], noninteracting SAW's describe the universal behavior of homopolymers in dilute solutions above the $\Theta$ temperature. In the polymer context, however, it is more interesting to consider a different model with medium-range interactions. Supposing, for simplicity, to be in the continuum (off-lattice), we can define a SAW in the following way. A SAW with medium range interactions is a collection of point $\{\omega_0, \ldots, \omega_n\}$, $\omega_i \in \mathbb{R}^d$, such that $|\omega_i - \omega_{i+1}| = \rho$ and $|\omega_i - \omega_j| > a$ for all $i \neq j$. In this case, the relevant scale is $\rho/a$ and the crossover limit is obtained for $\rho/a \to \infty$, $n \to \infty$, with $\tilde{n} \equiv n(\rho/a)^{-2d/(4-d)}$ fixed. For this model, the critical crossover functions can also be computed using Eq. (74), although with different nonuniversal $\rho$-independent constants $\lambda_E$, $\lambda_c$, and $\rho$. Thus, the results presented here are relevant for the description of polymeric systems in which the macromolecular persistence is much larger than the molecular scale. In practice, we expect the description to be reasonably accurate when $\rho/a \gtrsim 3$.

## APPENDIX A: CRITICAL CROSSOVER FUNCTIONS FROM FIELD THEORY

In this appendix, we will compute the critical crossover functions for the polymer case using field-theory methods. In Appendix A 1, we will use the approach of Refs. [28,29], while in Appendix A 2 we will present the results obtained using the method of Refs. [43,31,32]. The first approach provides the most precise estimates and it will be applied in Appendix A 3 to obtain numerical results for polymers generalizing Ref. [40].

### 1. Crossover functions in the fixed-dimension expansion

#### a. General results

In this section we report the critical crossover functions using the approach of Refs. [28,29]. We start from the expressions for $F_\chi(\tilde{t})$ and $F_\xi(\tilde{t})$:

$$F_\chi(\tilde{t}) = \chi^* \exp\left[ -\int_{y_0}^g dx \, \frac{\gamma(x)}{\nu(x) W(x)} \right], \quad \text{(A1)}$$

$$F_\xi(\tilde{t}) = (\xi^*)^2 \exp\left[ -2\int_{y_0}^g dx \, \frac{1}{W(x)} \right], \quad \text{(A2)}$$

where $\tilde{t}$ is related to the zero-momentum four-point renormalized coupling $g$ by

$$\tilde{t} = -t_0 \int_g^{g^*} dx \, \frac{\gamma(x)}{\nu(x) W(x)} \exp\left[ \int_{y_0}^x dz \, \frac{1}{\nu(z) W(z)} \right], \quad \text{(A3)}$$

$\gamma(x)$, $\nu(x)$, and $W(x)$ are the standard renormalization-group (RG) functions, $g^*$ is the critical value of $g$ defined by $W(g^*) = 0$, and $\chi^*$, $\xi^*$, $t_0$, and $y_0$ are normalization constants.

The expressions (A1), (A2), and (A3) are valid for any dimension $d < 4$. The first two equations are always well defined, while Eq. (A3) has been obtained with the additional hypothesis that the integral over $x$ is well defined when the integration is extended up to $g^*$. This hypothesis is verified when the system becomes critical at a finite value of $\beta$ and shows a standard critical behavior. In our case, $N = 0$, this is true for all $1 \leq d < 4$.

We normalize the coupling $g$ as in Refs. [66,89] so that in the perturbative limit $g \to 0, t \to \infty$, we have

$$g \approx \frac{4}{3(4\pi)^{d/2}} \Gamma\left(2 - \frac{d}{2}\right) \tilde{t}^{(d-4)/2} \equiv \lambda_d \tilde{t}^{(d-4)/2}. \quad \text{(A4)}$$

This implies that for $y_0 \to 0$, we have $t_0 \approx (y_0/\lambda_d)^{2/(d-4)}$ and $(\xi^*)^2 t_0 \approx \chi^* t_0 \approx 1$. With this normalization, in three dimensions the previous equations can be written as

$$F_\chi(\tilde{t}) = (6\pi g)^2 \exp\left[ -\int_0^g dx \left( \frac{\gamma(x)}{\nu(x) W(x)} + \frac{2}{x} \right) \right], \quad \text{(A5)}$$

$$F_\xi(\tilde{t}) = (6\pi g)^2 \exp\left[ -2\int_0^g dx \left( \frac{1}{W(x)} + \frac{1}{x} \right) \right], \quad \text{(A6)}$$

and

$$\tilde{t} = \frac{1}{(6\pi g)^2} \left( 1 - \frac{3g}{2} + \frac{g^2}{4} \log_{10} g \right) + D_3 + \frac{1}{(6\pi)^2} \int_0^g \frac{dx}{x^2}$$

$$\times \left\{ \frac{\gamma(x)}{\nu(x) W(x)} \exp\left[ \int_0^x dz \left( \frac{1}{\nu(z) W(z)} + \frac{2}{z} \right) \right] + \frac{2}{x} - \frac{3}{2} - \frac{x}{4} \right\}, \quad \text{(A7)}$$

where $D_3$ is a nonperturbative constant given by

$$D_3 = -\frac{1}{(6\pi)^2} \left[ \frac{1}{(g^*)^2} - \frac{3}{2g^*} + \tfrac{1}{4} \ln g^* \right]$$

$$- \frac{1}{(6\pi)^2} \int_0^{g^*} \frac{dx}{x^2} \left\{ \frac{\gamma(x)}{\nu(x) W(x)} \right.$$

$$\times \exp\left[ \int_0^x dz \left( \frac{1}{\nu(z) W(z)} + \frac{2}{z} \right) \right] + \frac{2}{x} - \frac{3}{2} - \frac{x}{4} \right\}. \quad \text{(A8)}$$

Numerically, $D_3 = 0.002\,473(6)$. Expressions for a general $N$-vector model and in two dimensions can be found in Ref. [27].

For $\tilde{t} \to \infty$, in three dimensions we obtain

$$F_\chi(\tilde{t}) = \frac{1}{\tilde{t}}\left[1 + \frac{1}{12\pi}\tilde{t}^{-1/2} - \frac{1}{288\pi^2\tilde{t}}\ln(36\pi^2\tilde{t})\right.$$

$$\left. - \frac{59}{2592\pi^2}\frac{1}{\tilde{t}} + \frac{D_3}{\tilde{t}} + O(\tilde{t}^{-3/2}\ln\tilde{t})\right], \quad \text{(A9)}$$

$$F_\xi(\tilde{t}) = \frac{1}{\tilde{t}}\left[1 + \frac{1}{12\pi}\tilde{t}^{-1/2} - \frac{1}{288\pi^2\tilde{t}}\ln(36\pi^2\tilde{t})\right.$$

$$\left. - \frac{11}{468\pi^2}\frac{1}{\tilde{t}} + \frac{D_3}{\tilde{t}} + O(\tilde{t}^{-3/2}\ln\tilde{t})\right]. \quad \text{(A10)}$$

### b. Asymptotic behavior near the Wilson-Fisher point

Let us now compute the asymptotic behavior of the crossover functions for $\tilde{t} \to 0$. This requires the determination of the expansion of the various RG functions in the limit $g \to g^*$. As it has been extensively discussed in the literature [42,90–92,60,88,93–97], these functions are singular at $g = g^*$. General arguments predict a behavior of the form [91,95]

$$W(g) = -\omega(g^* - g) + w_1(g^* - g)^2 + w_2(g^* - g)^{\Delta_2/\Delta}$$

$$+ w_3(g^* - g)^{1+1/\Delta} + \cdots, \quad \text{(A11)}$$

$$\gamma(g) = \gamma + \gamma_1(g^* - g) + \gamma_2(g^* - g)^2 + \gamma_3(g^* - g)^{\Delta_2/\Delta}$$

$$+ \gamma_4(g^* - g)^{1/\Delta} + \cdots, \quad \text{(A12)}$$

$$\nu(g) = \nu + \nu_1(g^* - g) + \nu_2(g^* - g)^2 + \nu_3(g^* - g)^{\Delta_2/\Delta}$$

$$+ \nu_4(g^* - g)^{1/\Delta} + \cdots. \quad \text{(A13)}$$

This nonanalytic behavior makes the determination of the corrections extremely difficult. For instance, since one expects $\Delta_2/\Delta$ to be close to 2 [98], it is practically impossible to determine $w_1$ and $w_2$ in the $\beta$ function since these two terms are essentially degenerate. The only subleading coefficients that can be reliably determined are $\gamma_1$ and $\nu_1$. Indeed, since $\Delta \approx \frac{1}{2}$ and $\Delta_2/\Delta \approx 2$, the next-to-leading correction behaves as $(g^* - g) \approx 2$, so that $\gamma'(g)$ and $\nu'(g)$ should be reasonably smooth for $g \to g^*$.

The computation is straightforward and we only report the final results. The crossover functions can be expanded for $\tilde{t} \to 0$ as

$$F_\chi(\tilde{t}) = \chi_0\tilde{t}^{-\gamma}[1 + \chi_1\tilde{t}^\Delta + \chi_2\tilde{t} + \chi_3\tilde{t}^{\Delta_2} + \chi_4\tilde{t}^{2\Delta} + \cdots], \quad \text{(A14)}$$

$$F_\xi(\tilde{t}) = \xi_0^2\tilde{t}^{-2\nu}[1 + \xi_1\tilde{t}^\Delta + \xi_2\tilde{t} + \xi_3\tilde{t}^{\Delta_2} + \xi_4\tilde{t}^{2\Delta} + \cdots]. \quad \text{(A15)}$$

We obtain for the leading term and the first correction

$$\chi_0 = (6\pi g^*)^2\tilde{t}^\gamma \exp\left\{-\int_0^{g^*}dx\left[\frac{\gamma(x)}{\nu(x)W(x)} + \frac{2}{x}\right.\right.$$

$$\left.\left. + \frac{\gamma}{\Delta(g^* - x)}\right]\right\}, \quad \text{(A16)}$$

$$\xi_0^2 = (6\pi g^*)^2\tilde{t}^{2\nu}\exp\left\{-2\int_0^{g^*}dx\left[\frac{1}{W(x)} + \frac{1}{x}\right.\right.$$

$$\left.\left. + \frac{1}{\omega(g^* - x)}\right]\right\}, \quad \text{(A17)}$$

$$\chi_1 = -\frac{g^*\gamma_1}{\Delta(1+\Delta)}\tilde{t}^{-\Delta}, \quad \text{(A18)}$$

$$\xi_1 = -\frac{2g^*}{\gamma\Delta(1+\Delta)}\tilde{t}^{-\Delta}[\gamma\nu_1(1+\Delta) - \nu\gamma_1\Delta], \quad \text{(A19)}$$

where

$$\hat{t} = \frac{\gamma}{(6\pi g^*)^2}\exp\left\{\int_0^{g^*}dx\left[\frac{1}{\nu(x)W(x)} + \frac{2}{x} + \frac{1}{\Delta(g^* - x)}\right]\right\}. \quad \text{(A20)}$$

In order to estimate these constants, we use the seven-loop results of Ref. [60] and the resummation technique of Ref. [89]. Errors due to the resummation are determined by using the general procedure of Ref. [95]. In order to compute $\chi_0$ and $\xi_0^2$, we perform resummations keeping $g^*$, $\gamma$, $\nu$, and $\Delta$ as free parameters (the dependence on $\Delta$ cancels in $\chi_0$ and $\xi_0^2$ if one uses the explicit expression for $\tilde{t}$). We obtain finally

$$\chi_0 = 0.4216 \pm 0.0006 - 4(\gamma - 1.1575) - 0.1(g^* - 1.395), \quad \text{(A21)}$$

$$\xi_0^2 = 0.3565 \pm 0.0002 + 0.4(\gamma - 1.1575) - 0.1(g^* - 1.395)$$

$$- 8(\nu - 0.587\,58), \quad \text{(A22)}$$

$$\hat{t} = [0.99 \pm 0.004 + 0.9(\gamma - 1.1575) - 8(g^* - 1.395)$$

$$- 9(\Delta - 0.515)] \times 10^{-3}, \quad \text{(A23)}$$

where the first error is related to the uncertainty in the resummation, while the other terms indicate the variation of the estimate with changes in the values of the critical exponents and of $g^*$. To obtain the final results, we must decide which estimates to use for $\gamma$, $\nu$, $\Delta$, and $g^*$. In principle, we could use the values that have been determined from the resummation of the perturbative expansions in three dimensions [61], i.e., $g^* = 1.413 \pm 0.006$, $\gamma = 1.1596 \pm 0.0020$, $\nu = 0.5882 \pm 0.0011$, and $\Delta = 0.478 \pm 0.010$. However, we believe the Monte Carlo estimates of the critical exponents to be more reliable, and thus we have used the values reported in Eq. (20). The field-theoretic estimate of $g^*$ is probably

also not reliable since it differs from the estimates obtained using different methods. Indeed, from the $\epsilon$ expansion one estimates $g^*=1.396\pm0.020$ [99], while the extrapolation of exact-enumeration series gives $g^*=1.388\pm0.005$ [100]: One observes a systematic discrepancy, which we believe to be due to the nonanalytic structure of the $\beta$ function that is not properly taken into account in the analysis [101]. This problem should also appear in our analysis since we use the same resummation technique. In the reanalysis of Ref. [55] of the perturbative series for the exponent $\gamma$, it was shown that the systematic error could be reduced, obtaining field-theory estimates in close agreement with the Monte Carlo results, if one uses $g^*\approx1.395$. Therefore, we use $g^*=1.395\pm0.015$, where the error is such to include all estimates. Our final estimates are

$$\chi_0=0.4216\pm0.0029, \tag{A24}$$

$$\xi_0^2=0.3565\pm0.0016, \tag{A25}$$

$$\hat{t}=(0.99\pm0.21)\times10^{-3}. \tag{A26}$$

To compute $\chi_1$ and $\xi_1$, we analyze the series of the derivative of $\gamma(g)$ and $\nu(g)$. We obtain

$$\gamma_1=-\gamma'(g^*)=-0.1071\pm0.0013+0.007(g^*-1.395), \tag{A27}$$

$$\nu_1=-\nu'(g^*)=-0.0659\pm0.0018-0.011(g^*-1.395). \tag{A28}$$

The ratio $\gamma_1/\nu_1$ has already been computed in Ref. [60] finding

$$\frac{\gamma_1}{\nu_1}=1.31\pm0.05-1.7(g^*-1.39), \tag{A29}$$

which, however, differs significantly from our result,

$$\frac{\gamma_1}{\nu_1}=1.62\pm0.05-0.4(g^*-1.395). \tag{A30}$$

Using the estimates of the critical exponents reported in Eq. (20) and, as before, $g^*=1.395\pm0.015$, we obtain

$$\chi_1=6.8\pm0.8, \tag{A31}$$

$$\xi_1=9.1\pm1.1. \tag{A32}$$

Notice that a significant fraction of the error is due to the uncertainty on $\hat{t}$. The error is largely reduced if we consider the ratio $\chi_1/\xi_1$. We obtain

$$\frac{\chi_1}{\xi_1}=0.745\pm0.034. \tag{A33}$$

Notice that, if we use the estimate (A29), we would obtain $\chi_1/\xi_1\approx0.56$. The ratio $\chi_1/\xi_1$ can also be computed in the $\epsilon$ expansion using the $O(\epsilon^2)$ series of Ref. [102]:

$$\frac{\chi_1}{\xi_1}=1-\frac{\epsilon}{8}-\left(\frac{\lambda}{12}+\frac{31}{256}\right)\epsilon^2+O(\epsilon^3), \tag{A34}$$

where $\lambda\approx1.171\,854$. We obtain $\chi_1/\xi_1=0.85\pm0.10$, where the error is purely indicative because of the shortness of the series.

### 2. Crossover functions in dimensional regularization without $\epsilon$ expansion

#### a. General results

In this section, we will study the critical crossover functions using the minimal renormalization scheme proposed in Refs. [43,31,32]. We start from the expressions [31,32]

$$F_\chi(\tilde{t})=\chi^*F(u)^{-1}\exp\left[-\int_{u_i}^u dx\,\frac{\gamma_M(x)}{\nu_M(x)W_M(x)}\right], \tag{A35}$$

$$F_\xi(\tilde{t})=(\xi^*)^2\exp\left[-2\int_{u_i}^u dx\,\frac{1}{W_M(x)}\right], \tag{A36}$$

where $\tilde{t}$ is related to the minimal-subtraction renormalized coupling $u$ by

$$\tilde{t}=-t_0\int_u^{u^*}dx\,\frac{2P(x)}{W_M(x)}\exp\left[\int_{u_i}^x dz\,\frac{1}{\nu_M(z)W_M(z)}\right]. \tag{A37}$$

Here $\gamma_M(x)$, $\nu_M(x)$, and $W_M(x)$ are the standard RG functions computed in dimensional regularization, $P(x)$ and $F(x)$ are functions defined in Refs. [31,32] that will be explicitly given below, and $u^*$ is the critical value of $u$ defined by $W_M(u^*)=0$. The constants $\chi^*$, $\xi^*$, $t_0$, and $u_i$ are obtained by requiring that, for $\tilde{t}\to0$, $F_x(\tilde{t})$ and $F_\xi(\tilde{t})$ behave as in Eq. (59). The RG functions have been computed to five-loop order in Refs. [69,70]. Explicitly, we have [103]

$$W_M(u)=W_M(u,1), \tag{A38}$$

$$\nu_M(u)=\frac{1}{2+\eta_2(u)}, \tag{A39}$$

$$\gamma_M(u)=[2-\eta_3(u)]\nu_M(u), \tag{A40}$$

where

$$W_M(u,\epsilon) = -\epsilon u + \tfrac{4}{3}u^2 - \tfrac{7}{6}u^3 + \frac{2960 + 2112\zeta(3)}{1728}u^4 + \frac{-196648 + 2816\pi/5 - 223872\zeta(3) - 357120\zeta(5)}{62208}u^5$$

$$+ \frac{13177344 - 67584\pi^4 - 317440\pi^6/21 + 21029376\zeta(3) + 2506752\zeta(3)^2 + 42261504\zeta(5) + 59383296\zeta(7)}{1990656}u^6$$

$$+ O(u^7), \tag{A41}$$

$$\eta_2(u) = -\tfrac{1}{3}u + \tfrac{5}{36}u^2 - \frac{37}{144}u^3 - \frac{-31060 - 352\pi^4/5 - 3264\zeta(3)}{62208}u^4$$

$$- \frac{3166528 + 42688\pi^4/5 + 39680\pi^6/21 + 1528704\zeta(3) - 446976\zeta(3)^2 + 55296\zeta(5)}{2985984}u^5 + O(u^6), \tag{A42}$$

$$\eta_3(u) = \tfrac{1}{36}u^2 - \tfrac{1}{108}u^3 + \tfrac{125}{5184}u^4 + \frac{-77056 - 1408\pi^4/5 + 8832\zeta(3)}{1492992}u^5 + O(u^6). \tag{A43}$$

To compute the functions $P(u)$ and $F(u)$, let us first recall the relation between the bare coupling $u_0$ and the renormalized coupling $u$,

$$u_0 = \mu A_3^{-1} u Z_u(u) Z_\varphi(u)^{-2}, \tag{A44}$$

$$Z_u(u) Z_\varphi(u)^{-2} = \exp\left\{ -\int_0^u du' \left[ \frac{1}{W_M(u')} + \frac{2}{u'} \right] \right\}. \tag{A45}$$

Here $\mu$ is the renormalization scale and $A_d$ is a constant that depends on the specific renormalization scheme. Of course, physical results should not depend on it. This fact can be easily verified by noticing that $A_d$ can be absorbed in the definition of $\mu$, and that, by construction, all physical quantities are independent of $\mu$. However, different choices of $A_d$ give rise to different perturbative series providing different results at the intermediate stages of the calculation. This freedom may be used as a further check of the uncertainty of the final results. In Refs. [31,32] the authors use

$$A_d = S_d \Gamma(3 - d/2) \Gamma(d/2 - 1), \tag{A46}$$

$$S_d = \frac{2}{(4\pi)^{d/2} \Gamma(d/2)},$$

a choice that makes the one-loop corrections vanish in many observables. However, in order to understand the size of the systematic errors, we will also use $A_d = S_d$ and $A_d = 4S_d$.

The functions $F(u)$ and $P(u)$ are obtained from

$$F(u) \equiv Z_\varphi(u) F_0[A_3^{-1} u Z_u(u) Z_\varphi(u)^{-2}], \tag{A47}$$

$$Z_\varphi(u) = \exp\left[ \int_0^u du' \frac{\eta_3(u')}{W_M(u')} \right], \tag{A48}$$

and

$$P(u) \equiv Z_{\varphi^2}(u)^{-1} P_0[A_3^{-1} u Z_u(u) Z_\varphi(u)^{-2}], \tag{A49}$$

$$Z_{\varphi^2}(u) = \exp\left[ \int_0^u du' \frac{\eta_2(u')}{W_M(u')} \right], \tag{A50}$$

where $F_0(x)$ and $P_0(x)$ can be derived from the five-loop results of Refs. [29,32]:

$$F_0(x) = 1 + \frac{1}{7776\pi^2}x^2 - 8.83291 \times 10^{-7}x^3$$

$$+ 6.17241 \times 10^{-8}x^4$$

$$- 4.73993 \times 10^{-9}x^5 + O(x^6), \tag{A51}$$

$$P_0(x) = 1 + \frac{1}{24\pi}x - \frac{1}{288\pi^2}x^2 + 1.81785 \times 10^{-5}x^3$$

$$- 1.24518 \times 10^{-6}x^4$$

$$+ 1.01097 \times 10^{-7}x^5 + O(x^6). \tag{A52}$$

When $A_d$ is given by Eq. (A46), we have

$$F(u) = 1 - \tfrac{23}{1944}u^2 - 5.525\,10 \times 10^{-3}u^3 - 4.016\,33 \times 10^{-3}u^4$$

$$- 1.929\,54 \times 10^{-3}u^5 + O(u^6), \tag{A53}$$

$$P(u) = 1 - \tfrac{1}{6}u + \tfrac{1}{72}u^2 - 0.031\,827\,9u^3 + 0.032\,666\,4u^4$$

$$- 0.064\,406\,5u^5 + O(u^6). \tag{A54}$$

**b. Asymptotic behavior near the Wilson-Fisher point**

In order to compute the asymptotic behavior of the crossover functions for $\tilde{t} \to 0$, we need the expansion of the various RG functions in the limit $u \to u^*$. It has been argued [104] that the scheme we are presenting has an important advantage over the approach described in Appendix A 1: The RG functions are expected to be analytic at the critical point. The reason is that the RG functions are essentially dimension-independent, while $u^*$ depends on $\epsilon$ being the solution of $W_M(u^*, \epsilon) = 0$. Notice, however, that this argu-

ment does not exclude the presence of singular terms for $u = 0$ since this scheme is essentially four-dimensional. Answering this question is in any case nontrivial since it requires a nonperturbative definition of the RG functions. In the following we will assume the following analytic expansions:

$$W_M(u) = -\omega(u^* - u) + w_1(u^* - u)^2 + \cdots, \quad \text{(A55)}$$

$$\gamma_M(u) = \gamma + \gamma_1(u^* - u) + \cdots, \quad \text{(A56)}$$

$$\nu_M(u) = \nu + \nu_1(u^* - u) + \cdots, \quad \text{(A57)}$$

$$F(u) = f^* + f_1(u^* - u) + \cdots, \quad \text{(A58)}$$

$$P(u) = p^* + p_1(u^* - u) + \cdots. \quad \text{(A59)}$$

Expanding the crossover functions for $\tilde{t} \to 0$ as in Eqs. (A14) and (A15), we obtain the following for the leading term and the first correction:

$$\chi_0 = \frac{(\kappa u^*)^2}{f^*} \hat{t}^\gamma \exp\left\{ -\int_0^{u^*} dx \left[ \frac{\gamma_M(x)}{\nu_M(x) W_M(x)} + \frac{2}{x} \right.\right.$$

$$\left.\left. + \frac{\gamma}{\Delta(u^* - x)} \right] \right\}, \quad \text{(A60)}$$

$$\xi_0^2 = (\kappa u^*)^2 \hat{t}^{2\nu} \exp\left\{ -2 \int_0^{u^*} dx \left[ \frac{1}{W_M(x)} + \frac{2}{x} \right.\right.$$

$$\left.\left. + \frac{1}{\omega(u^* - x)} \right] \right\}, \quad \text{(A61)}$$

$$\chi_1 = -u^* \left[ \frac{f_1}{f^*} + \frac{\gamma_1}{\Delta} - \frac{\gamma}{1 + \Delta} \left( \frac{\nu_1}{\nu} + \frac{p_1}{p^*} \right) \right] \hat{t}^{-\Delta}, \quad \text{(A62)}$$

$$\xi_1 = u^* \frac{2\nu}{1 + \Delta} \left( \frac{p_1}{p^*} - \frac{\nu_1}{\Delta\nu} \right) \hat{t}^{-\Delta}, \quad \text{(A63)}$$

where

$$\hat{t} = \frac{2p^*\nu}{(\kappa u^*)^2} \exp\left\{ \int_0^{u^*} dx \left[ \frac{1}{\nu_M(x) W_M(x)} + \frac{1}{x} + \frac{1}{\Delta(u^* - x)} \right] \right\}. \quad \text{(A64)}$$

The normalization $\kappa$ is related to the choice of $A_d$ in Eq. (A45) by

$$\kappa = 4\pi(1 + 2q_3),$$

$$q_d = \frac{S_d \Gamma(3 - d/2) \Gamma(d/2 - 1) - A_d}{2(4 - d) A_d}. \quad \text{(A65)}$$

The estimate of critical quantities requires a resummation of the perturbative series. For this purpose we will use the large-order behavior of the coefficients [105,106] given by

$$c_k \sim k! (-\tfrac{1}{2})^k k^b [1 + O(1/k)], \quad \text{(A66)}$$

and the numerical method of Refs. [89,95].

We have first of all determined $u^*$. We obtain $u^* = 1.1 \pm 0.1$. Although this result is consistent with the estimate of Ref. [31], $u^* = 1.092 \pm 0.012$, the error bar is much larger. However, using our algorithm [95], we have been unable to understand how the error can be so small. On the other hand, as we shall see later by comparing our results with the estimates of the preceding section and by checking their independence on $A_d$, our error bars look reasonable and at most overestimated by a factor of 2. In the following, we report various estimates keeping $u^*$ as a free variable. We have

$$\gamma_1 = -0.140 \pm 0.010 - 0.01(u^* - 1.1), \quad \text{(A67)}$$

$$\nu_1 = -0.089 \pm 0.010 - 0.02(u^* - 1.1), \quad \text{(A68)}$$

$$f^* = \begin{cases} 0.991 \pm 0.004 - 0.02(u^* - 1.1) \\ 0.987 \pm 0.006 - 0.02(u^* - 1.1) \\ 0.983 \pm 0.006 - 0.02(u^* - 1.1), \end{cases} \quad \text{(A69)}$$

$$p^* = \begin{cases} 0.932 \pm 0.006 - 0.05(u^* - 1.1) \\ 0.825 \pm 0.015 - 0.15(u^* - 1.1) \\ 0.670 \pm 0.040 - 0.30(u^* - 1.1), \end{cases} \quad \text{(A70)}$$

$$f_1 = \begin{cases} 0.026 \pm 0.007 + 0.03(u^* - 1.1) \\ 0.039 \pm 0.012 + 0.04(u^* - 1.1) \\ 0.051 \pm 0.018 + 0.06(u^* - 1.1), \end{cases} \quad \text{(A71)}$$

$$p_1 = \begin{cases} 0.0749 \pm 0.015 + 0.03(u^* - 1.1) \\ 0.182 \pm 0.012 + 0.02(u^* - 1.1) \\ 0.399 \pm 0.030 + 0.13(u^* - 1.1). \end{cases} \quad \text{(A72)}$$

For $f^*$, $p^*$, $f_1$, and $p_1$ we report three estimates corresponding to $A_3 = S_3$, $1/4\pi$, and $4S_3$, respectively. Notice that in most cases the uncertainty on $u^*$ is negligible compared to the resummation errors. We obtain finally

$$\chi_0 = 0.420(15), 0.422(19), 0.447(42), \quad \text{(A73)}$$

$$\xi_0^2 = 0.358(15), 0.363(19), 0.395(38), \quad \text{(A74)}$$

$$\chi_1 = 6.7(4.2), 6.5(4.1), 5.4(3.4), \quad \text{(A75)}$$

$$\xi_1 = 10.1(6.3), 9.2(5.7), 6.7(4.2), \quad \text{(A76)}$$

where the three different estimates correspond to $A_3 = S_3$, $1/4\pi$, and $4S_3$, respectively. As before, a more precise estimate is obtained if one considers $\chi_1/\xi_1$. We obtain

$$\frac{\chi_1}{\xi_1} = 0.66(13), 0.71(10), 0.81(7). \quad \text{(A77)}$$

As expected, these results are independent of the value of $A_3$ within error bars. Notice that the difference among the estimates of the same quantity is of the same order of the error bars, thereby confirming the correctness of our error estimates. The final results are also in good agreement with, although less precise than, the results presented in the preceding section. Notice that the estimate of $\chi_1/\xi_1$ obtained

here is compatible with the estimate obtained in Appendix A 1 b. Instead, the result of Ref. [60] is somewhat too small.

### 3. Polymer critical crossover functions

Let us now compute the critical crossover functions in terms of $\tilde{n}$. We will only consider the approach described in Appendix A 1, since it appears to be the most precise one. From Eq. (40) we have

$$G_c(\tilde{n}) = \int_{c-i\infty}^{c+i\infty} \frac{d\tilde{t}}{2\pi i} e^{\tilde{n}\tilde{t}} F_\chi(\tilde{t}). \tag{A78}$$

Changing variables from $\tilde{t}$ to $g$, we obtain

$$G_c(\tilde{n}) = \chi^* t_0 \int_C \frac{dg}{2\pi i} e^{\tilde{n}\tilde{t}(g)} \frac{\gamma(g)}{\nu(g)W(g)}$$

$$\times \exp\left[\int_{y_0}^g dz \frac{1-\gamma(z)}{\nu(z)W(z)}\right], \tag{A79}$$

where $C$ may be taken as a circle of the form $g=R(1+e^{-i\phi})$, $-\pi \leq \phi \leq \pi$, with $R$ fixed satisfying $0<R<g^*/2$.

To compare with the results of Ref. [40] we introduce their notations,

$$\beta(g) = \frac{2\nu(g)W(g)}{\gamma(g)}, \tag{A80}$$

$$j(g) = 2\left(1 - \frac{1}{\gamma(g)}\right), \tag{A81}$$

$$J(g) = \left(1 - \frac{g}{g^*}\right)^{(1-\gamma)/\Delta} \exp\left\{-\int_0^g dx\left[\frac{j(x)}{\beta(x)} + \frac{\gamma-1}{\Delta(g^*-x)}\right]\right\}, \tag{A82}$$

$$A(g) = \exp\left\{\int_0^g dx\left[\frac{2-j(x)}{\beta(x)} + \frac{2}{x} + \frac{1}{\Delta(g^*-x)}\right]\right\}, \tag{A83}$$

$$E_0(g) = \int_{g^*}^g dx\left(1 - \frac{x}{g^*}\right)^{1/\Delta} \frac{A(x)}{x^2\beta(x)}, \tag{A84}$$

where $\gamma$ and $\Delta$ are the standard critical exponents. Then, we obtain

$$G_c(\tilde{n}) = 2\int_C \frac{dg}{2\pi i} \frac{J(g)}{\beta(g)} \exp\left[\frac{\tilde{n}}{18\pi^2} E_0(g)\right]. \tag{A85}$$

In order to have the same definitions of Refs. [39,40], let us also introduce

$$z = \frac{\sqrt{\tilde{n}}}{24\pi^{3/2}}. \tag{A86}$$

We obtain finally

$$G_c(z) = \int_C \frac{dg}{\pi i} \frac{J(g)}{\beta(g)} e^{32\pi z^2 E_0(g)} \tag{A87}$$

Expanding the previous expression for $z \to 0$, we obtain the perturbative expansion (68).

The computation of $G_E(z)$ is analogous. Starting from

$$G_E(\tilde{n}) = \frac{1}{G_c(\tilde{n})} \int_{c-i\infty}^{c+i\infty} \frac{d\tilde{t}}{2\pi i} e^{\tilde{n}\tilde{t}} F_\chi(\tilde{t}) F_\xi(\tilde{t}), \tag{A88}$$

we obtain for the swelling factor [40] $S_E(z) = G_E(z)/(6\tilde{n})$,

$$S_E(z) = \frac{1}{16\pi z^2 G_0(z)} \int_C \frac{dg}{\pi i} \frac{J(g)K(g)}{\beta(g)E(g)} e^{32\pi z^2 E_0(g)}, \tag{A89}$$

where

$$k(g) = 2\left(\frac{2\nu(g)}{\gamma(g)} - 1\right), \tag{A90}$$

$$K(g) = \left(1 - \frac{g}{g^*}\right)^{(\gamma-2\nu)/\Delta}$$

$$\times \exp\left\{-\int_0^g dx\left[\frac{k(x)}{\beta(x)} + \frac{\gamma-2\nu}{\Delta(g^*-x)}\right]\right\}, \tag{A91}$$

$$E(g) = \frac{1}{g^2}\left(1 - \frac{g}{g^*}\right)^{\gamma/\Delta} \exp\left\{2\int_0^g dx\left[\frac{1}{\beta(x)} + \frac{1}{x}\right.\right.$$

$$\left.\left. + \frac{\gamma}{2\Delta(g^*-x)}\right]\right\}. \tag{A92}$$

From the previous expressions we can compute the asymptotic behavior of $G_c(z)$ and $S_E(z)$ for $z \to \infty$. We have

$$G_c(z) = g_{c0}z^{2(\gamma-1)}(1 + g_{c1}z^{-2\Delta} + g_{c2}z^{-2} + g_{c3}z^{-2\Delta_2} + \cdots), \tag{A93}$$

$$S_E(z) = s_{E0}z^{4\nu-2}(1 + s_{E1}z^{-2\Delta} + s_{E2}z^{-2} + s_{E3}z^{-2\Delta_2} + \cdots). \tag{A94}$$

These expansions can be related to the expansions of $F_\chi(\tilde{t})$ and $F_\xi(\tilde{t})$ for $\tilde{t} \to 0$. Using the results of Appendix A 1 b, we have

$$g_{c0} = \frac{\chi_0}{\Gamma(\gamma)}(24\pi^{3/2})^{2(\gamma-1)} = 2.117 \pm 0.020, \tag{A95}$$

$$s_{E0} = \frac{\xi_0^2\Gamma(\gamma)}{\Gamma(\gamma+2\nu)}(24\pi^{3/2})^{2(2\nu-1)} = 1.549 \pm 0.007, \tag{A96}$$

$$g_{c1} = \frac{\chi_1\Gamma(\gamma)}{\Gamma(\gamma-\Delta)}(24\pi^{3/2})^{-2\Delta} = 0.029 \pm 0.005, \tag{A97}$$

$$s_{E1} = \left[\frac{(\chi_1+\xi_1)\Gamma(\gamma+2\nu)}{\Gamma(\gamma+2\nu-\Delta)} - \frac{\chi_1\Gamma(\gamma)}{\Gamma(\gamma-\Delta)}\right](24\pi^{3/2})^{-2\Delta}$$

$$= 0.101 \pm 0.016. \tag{A98}$$

If we consider the ratio $g_{c1}/s_{E1}$, the error is largely reduced and we have

$$\frac{g_{c1}}{s_{E1}} = 0.288 \pm 0.016. \qquad (A99)$$

The constants $s_{E0}$ and $s_{E1}$ have already been computed in Ref. [40], finding $s_{E0} \approx 1.5310$ and $s_{E1} \approx 0.1204$, in reasonable agreement with our results. The constants $s_{E0}$ and $s_{E1}$ have also been determined by a Monte Carlo simulation of the Domb-Joyce model [54], obtaining

$$s_{E0} = \lim_{\omega \to 0} B_R(\omega) \approx 1.546\,54, \qquad (A100)$$

$$s_{E1} = \lim_{\omega \to 0} b_R(\omega) \approx 0.114\,98, \qquad (A101)$$

where $B_R(\omega)$ and $b_R(\omega)$ are defined in Ref. [54].

We have computed the functions $G_c(z)$ and $S_E(z)$ using the numerical technique presented in Ref. [40]. In the resummation we have used the seven-loop results of Ref. [60] that allow the extension of the series expansions of $j(g)$ and $k(g)$ by one order. If

$$j(g) = \sum_n j_n g^n, \quad k(g) = \sum_n k_n g^n, \qquad (A102)$$

we derive from Ref. [60]

$$j_7 = 0.099\,688\,8, \quad k_7 = -0.001\,906\,71. \qquad (A103)$$

The results for $G_c(z)$ are well fitted by

$$G_c(z) = (1 + 50.793\,65z + 508.5428z^2 + 5929.475z^3$$
$$+ 10\,937.03z^4)^{0.07875}. \qquad (A104)$$

For $z \to 0$, this expression gives $G_c(z) \approx 1 + 4z$, in agreement with the perturbative expansion (68), while for $z \to \infty$ we have

$$G_c(z) = 2.08z^{2\gamma-2}[1 + 0.089z^{-1} + O(z^{-2})]. \qquad (A105)$$

This expansion is in reasonable agreement with Eq. (A93), keeping into account that $\Delta \approx \frac{1}{2}$. However, while the leading term is close to the estimate (A95), the correction differs significantly from Eq. (A97). A simpler expression, that is, however, more accurate in the Wilson-Fisher region, is

$$G_c(z) = (1 + 38.0952z + 276.844z^2 + 1073.17z^3)^{0.105}. \qquad (A106)$$

For $z \to \infty$, it behaves as

$$G_c(z) \approx 2.08z^{2\gamma-2}(1 + 0.027z^{-1}), \qquad (A107)$$

in agreement with the asymptotic expansion (A93) and the numerical values (A95) and (A97).

For $S_E(z)$ we find that the expression reported in Ref. [54],

$$S_E(z) = (1 + 7.6118z + 12.051\,35z^2)^{0.175\,166}, \qquad (A108)$$

fits the data extremely well and correctly reproduces the asymptotic behavior for $z \to 0$ and $z \to \infty$. A different interpolation appears in Ref. [104], based on the five-loop computations of Schloms and Dohm [31]. Setting $z = 6.95\bar{z}$ in the formulas of Ref. [104] in order to reproduce the correct behavior for $z \to 0$, we obtain

$$S_E(z) = (1 + 7.4074z + 10.913z^2)^{0.18}, \qquad (A109)$$

in good agreement with Eq. (A108). Another interpolation formula was proposed in Ref. [9], motivated again by perturbative field theory. The swelling factor $S_E(z)$ is obtained by solving the equation

$$S_E(z)^{2.8215} - S_E(z)^{0.1975} = 3.3261z. \qquad (A110)$$

Other phenomenological representations are reported in Refs. [40], [107], [75].

Finally, from the results reported in Ref. [58], we can estimate the ratio $g_{c1}/s_{E1}$. We find $g_{c1}/s_{E1} \approx 0.26$, in reasonable agreement with Eq. (A99). Let us finally notice that if we use the estimate (A29) we would obtain $g_{c1}/s_{E1} \approx 0.23$.

[1] *Phase Transitions: Cargèse 1980*, edited by M. Lévy, J. C. Le Guillou, and J. Zinn-Justin (Plenum, New York, 1981).

[2] A. Pelissetto and E. Vicari, e-print cond-mat/0012164.

[3] V. L. Ginzburg, Fiz. Tverd. Tela (Leningrad) **2**, 2031 (1960) [Sov. Phys. Solid State **2**, 1824 (1960)].

[4] Z. Y. Chen, P. C. Albright, and J. V. Sengers, Phys. Rev. A **41**, 3161 (1990).

[5] Z. Y. Chen, A. Abbaci, S. Tang, and J. V. Sengers, Phys. Rev. A **42**, 4470 (1990).

[6] S. B. Kiselev, I. G. Kostyukova, and A. A. Povodyrev, Int. J. Thermophys. **12**, 877 (1991).

[7] M. A. Anisimov, S. B. Kiselev, J. V. Sengers, and S. Tang, Physica A **188**, 487 (1992).

[8] M. Y. Belyakov and S. B. Kiselev, Physica A **190**, 75 (1992).

[9] Z. Y. Chen and J. Noolandi, J. Chem. Phys. **96**, 1540 (1992).

[10] G. X. Jin, S. Tang, and J. V. Sengers, Phys. Rev. E **47**, 388 (1993).

[11] A. Kostrowicka Wyczalkowska, M. A. Anisimov, and J. V. Sengers, Fluid Phase Equilibria **158-160**, 523 (1999).

[12] M. A. Anisimov and J. V. Sengers, in *Supercritical Fluids—Fundamentals and Applications*, edited by E. Kiran, P. G. Debenedetti, and C. J. Peters (Kluwer, Dordrecht, 2000), p. 89.

[13] M. A. Anisimov and J. V. Sengers, in *Equations of State for Fluids and Fluid Mixtures*, edited by J. V. Sengers, R. F. Kayser, C. J. Peters, and H. J. White, Jr. (Elsevier, Amster-

dam, 2000), p. 381.

[14] S. B. Kiselev and J. F. Ely, Fluid Phase Equilibria **174**, 93 (2000).

[15] K. Binder, E. Luijten, M. Müller, N. B. Wilding, and H. W. J. Blöte, Physica A **281**, 112 (2000).

[16] E. Luijten and H. Meyer, Phys. Rev. E **62**, 3257 (2000).

[17] L. Lue and S. B. Kiselev, J. Chem. Phys. **114**, 5026 (2001).

[18] V. A. Agayan, M. A. Anisimov, and J. V. Sengers, Phys. Rev E **64**, 026125 (2001).

[19] K. K. Mon and K. Binder, Phys. Rev. E **48**, 2498 (1993).

[20] E. Luijten, H. W. J. Blöte, and K. Binder, Phys. Rev. E **54**, 4626 (1996).

[21] E. Luijten, H. W. J. Blöte, and K. Binder, Phys. Rev. Lett. **79**, 561 (1997); Phys. Rev. E **56**, 6540 (1997).

[22] E. Luijten and K. Binder, Phys. Rev. E **58**, R4060 (1998); **59**, 7254 (1999); Europhys. Lett. **47**, 311 (1999).

[23] E. Luijten, Phys. Rev. E **59**, 4997 (1999).

[24] G. Orkoulas, A. Z. Panagiotopoulos, and M. E. Fisher, Phys. Rev. E **61**, 5930 (2000).

[25] J. S. Kouvel and M. E. Fisher, Phys. Rev. **136**, A1626 (1964).

[26] A. Pelissetto, P. Rossi, and E. Vicari, Phys. Rev. E **58**, 7146 (1998).

[27] A. Pelissetto, P. Rossi, and E. Vicari, Nucl. Phys. B **554**, 552 (1999).

[28] C. Bagnuls and C. Bervillier, J. Phys. (France) Lett. **45**, L-95 (1984).

[29] C. Bagnuls and C. Bervillier, Phys. Rev. B **32**, 7209 (1985).

[30] C. Bagnuls, C. Bervillier, D. I. Meiron, and B. G. Nickel, Phys. Rev. B **35**, 3585 (1987); e-print hep-th/0006187.

[31] R. Schloms and V. Dohm, Nucl. Phys. B **328**, 639 (1989).

[32] H. J. Krause, R. Schloms, and V. Dohm, Z. Phys. B: Condens. Matter **79**, 287 (1990).

[33] P. G. de Gennes, Phys. Lett. **38A**, 339 (1972).

[34] M. Daoud, J. P. Cotton, B. Farnoux, G. Jannink, G. Sarma, H. Benoit, R. Duplessix, C. Picot, and P. G. de Gennes, Macromolecules **8**, 804 (1975).

[35] V. J. Emery, Phys. Rev. B **11**, 239 (1975).

[36] C. Aragão de Carvalho, S. Caracciolo, and J. Fröhlich, Nucl. Phys. B **215**, 209 (1983).

[37] P. G. de Gennes, *Scaling Concepts in Polymer Physics* (Cornell University Press, Ithaca, NY, 1980).

[38] J. des Cloizeaux and G. Jannink, *Les Polymères en Solution* (Les Editions de Physique, Les Ulis, 1987); English translation: *Polymers in Solution: Their Modeling and Structure* (Oxford University Press, Oxford, 1990).

[39] M. Muthukumar and B. G. Nickel, J. Chem. Phys. **80**, 5839 (1984).

[40] M. Muthukumar and B. G. Nickel, J. Chem. Phys. **86**, 460 (1987).

[41] J. des Cloizeaux, R. Conte, and G. Jannink, J. Phys. (France) Lett. **46**, L-595 (1985).

[42] G. Parisi, J. Stat. Phys. **23**, 49 (1980).

[43] V. Dohm, Z. Phys. B: Condens. Matter **60**, 61 (1985); **61**, 193 (1985).

[44] S. Caracciolo, M. S. Causo, A. Pelissetto, P. Rossi, and E. Vicari, Nucl. Phys. B (Proc. Suppl.) **73**, 757 (1999).

[45] For the general $N$-vector model in two dimensions, a critical point exists only for $N \leqslant 2$. Theories with $N \geqslant 3$ are asymptotically free and become critical only in the limit $\beta \rightarrow \infty$.

[46] B. Nienhuis, Phys. Rev. Lett. **49**, 1062 (1982); J. Stat. Phys. **34**, 731 (1984).

[47] A. J. Guttmann and I. G. Enting, J. Phys. A **21**, L165 (1988).

[48] H. Saleur, J. Phys. A **20**, 455 (1987).

[49] A. R. Conway and A. J. Guttmann, J. Phys. A **26**, 1535 (1993).

[50] A. R. Conway and A. J. Guttmann, Phys. Rev. Lett. **77**, 5284 (1996).

[51] I. Guim, H. W. J. Blöte, and T. W. Burkhardt, J. Phys. A **30**, 413 (1997).

[52] S. Caracciolo, M. S. Causo, P. Grassberger, and A. Pelissetto, J. Phys. A **32**, 2931 (1999).

[53] B. Li, N. Madras, and A. D. Sokal, J. Stat. Phys. **80**, 661 (1995).

[54] P. Belohorec and B. G. Nickel, Guelph University Report, Accurate universal and two-parameter model results from a Monte-Carlo renormalization group study, September 1997 (unpublished).

[55] S. Caracciolo, M. S. Causo, and A. Pelissetto, Phys. Rev. E **57**, R1215 (1998).

[56] N. Eizenberg and J. Klafter, J. Chem. Phys. **99**, 3976 (1993); Phys. Rev. B **53**, 5078 (1996).

[57] J. S. Pedersen, M. Laso, and P. Shurtenberger, Phys. Rev. E **54**, R5917 (1996).

[58] P. Grassberger, P. Sutter, and L. Schäfer, J. Phys. A **30**, 7039 (1997).

[59] G. Besold, H. Guo, and M. J. Zuckermann, J. Polym. Sci., Part B: Polym. Phys. **38**, 1053 (2000).

[60] D. B. Murray and B. G. Nickel, Guelph University Report, Accuurate universal and two-parameter model results from a Monte-Carlo renormalization group study (1991) (unpublished). The seven-loop perturbative series are reported in the Appendix of Ref. [61].

[61] R. Guida and J. Zinn-Justin, J. Phys. A **31**, 8103 (1998).

[62] J. Berges, N. Tetradis, and C. Wetterich, e-print hep-ph/0005122.

[63] F. Jasch and H. Kleinert, J. Math. Phys. **42**, 52 (2001).

[64] P. Butera and M. Comi, Phys. Rev. B **56**, 8212 (1997).

[65] D. MacDonald, S. Joseph, D. L. Hunter, L. L. Moseley, N. Jan, and A. J. Guttmann, J. Phys. A **33**, 5973 (2000).

[66] G. A. Baker, Jr., B. G. Nickel, M. S. Green, and D. I. Meiron, Phys. Rev. Lett. **36**, 1351 (1977); G. A. Baker, Jr., B. G. Nickel, and D. I. Meiron, Phys. Rev. B **17**, 1365 (1978).

[67] This behavior can be observed only for quantities that are defined using $R$ as a scale. If we were considering, for instance, $\chi_R(t)\rho^{-2d/(4-d)}$, we would of course obtain the same universal limiting curve, but now with corrections of order $1/\rho$.

[68] This behavior is correct for $2 < d < 4$. In two dimensions, the leading correction cannot be computed in a mean-field expansion and thus we do not have a theoretical prediction. However, numerical and theoretical arguments [20,21,27] indicate that the corrections should be of order $1/R^{-2}$ times powers of $\ln_{10} R$.

[69] K. G. Chetyrkin, S. G. Gorishny, S. A. Larin, and F. V. Tkachov, Phys. Lett. **132B**, 351 (1983).

[70] H. Kleinert, J. Neu, V. Schulte-Frohlinde, K. G. Chetyrkin, and S. A. Larin, Phys. Lett. B **272**, 39 (1991); **319**, 545(E) (1993).

[71] J. P. Eckmann, J. Magnen, and R. Sénéor, Commun. Math. Phys. **39**, 251 (1975).

[72] J. S. Feldman and K. Osterwalder, Ann. Phys. **97**, 80 (1976).

[73] J. Magnen and R. Sénéor, Commun. Math. Phys. **56**, 237 (1977).

[74] J. Magnen and V. Rivasseau, Commun. Math. Phys. **102**, 59 (1985).

[75] Other representations [108–112,41] for $G_E(\tilde{n}_{SR})$ are reviewed in Refs. [40,107]. Note that in Refs. [40,107], $\alpha^2$ stands for $G_E(\tilde{n}_{SR})/(6\tilde{n}_{SR})$.

[76] N. Madras and A. D. Sokal, J. Stat. Phys. **50**, 109 (1988).

[77] S. Caracciolo, A. Pelissetto, and A. D. Sokal, Nucl. Phys. B (Proc. Suppl.) **20**, 68 (1991); J. Stat. Phys. **67**, 65 (1992).

[78] Z. Alexandrowicz, J. Chem. Phys. **51**, 561 (1969).

[79] Z. Alexandrowicz and Y. Accad, J. Chem. Phys. **54**, 5538 (1971).

[80] P. Grassberger, Phys. Rev. E **56**, 3682 (1997); P. Grassberger and R. Hegger, J. Phys. I **5**, 597 (1995).

[81] The self-avoidance check can be performed in a CPU time of order 1 by using a hashing technique; see, e.g., Refs. [76,113].

[82] In order to compare with spin models, it is interesting to relate our values of $E_{n,R}^2$ with $\xi_R(\beta)$, where, for each $n$, we consider the value of $\beta$ such that $\langle n \rangle_\beta = n$. In the critical limit we find the relation

$$\xi_R(\beta)^2 = \frac{\Gamma(\gamma+2\nu)}{6\Gamma(\gamma)\gamma^{2\nu}} E_{n,R}^2.$$

Therefore, we reach $\xi \approx 35, 80, 300, 500, 350, 500, 500, 700, 700, 500$, respectively, for $\rho = 2, 3, 4, 5, 6, 7, 8, 9, 10, 12$.

[83] For $\rho = 2, 7, 12$, we have computed the observables for additional values of $n$, larger than the minimum value of $n$ reported in the table. More precisely, by using the SSA, we have computed the observables for all $n \leq 30, 400, 3000$, respectively.

[84] In principle, we could have used Eq. (72) for $G_c(z)$. However, here it is important to use an expression for $g_{c,\text{th}}(\tilde{n})$ which is precise in the Wilson-Fisher region. For this reason, we have chosen to use Eq. (A106).

[85] In the fits we also used estimates obtained by means of the SSA. In order to reduce the correlations and to avoid the fit being dominated by data with small values of $n$, we have used only some of them. We considered the values corresponding to $n = n_0 \lfloor e^{(k+k_0)/5} \rfloor$, $k \in \mathbb{N}$, where $\lfloor x \rfloor$ is the largest integer smaller than $x$ and $n_0$ and $k_0$ are integers.

[86] We assume $g_{c,\text{th}}(\tilde{n})$ to have an error of 0.3% for $\tilde{n} \gtrsim 1$, and of $0.3\tilde{n}$% for $\tilde{n} < 1$. The smaller error for $\tilde{n} < 1$ is due to the fact that our representation (72) has the exact leading behavior for $z \to 0$, cf. Sec. IV.

[87] M. A. Anisimov, E. Luijten, V. A. Agayan, J. V. Sengers, and K. Binder, Phys. Lett. A **264**, 63 (1999).

[88] B. G. Nickel, Macromolecules **24**, 1358 (1991).

[89] J. C. Le Guillou and J. Zinn-Justin, Phys. Rev. B **21**, 3976 (1980).

[90] G. Parisi, Phys. Lett. **76B**, 448 (1978); Phys. Rep. **49**, 215 (1979).

[91] B. G. Nickel, in *Phase Transitions, Cargèse 1981*, edited by M. Lévy, J. C. Le Guillou, and J. Zinn-Justin (Plenum, New York, 1982).

[92] B. G. Nickel, Physica A **117**, 189 (1991).

[93] A. D. Sokal, Europhys. Lett. **27**, 661 (1994).

[94] C. Bagnuls and C. Bervillier, J. Phys. Stud. **1**, 366 (1997).

[95] A. Pelissetto and E. Vicari, Nucl. Phys. B **519**, 626 (1998).

[96] P. Calabrese, M. Caselle, A. Celi, A. Pelissetto, and E. Vicari, J. Phys. A **33**, 8155 (2000).

[97] M. Caselle, A. Pelissetto, and E. Vicari, in *Fluctuating Paths and Fields*, edited by W. Janke, A. Pelster, H.-J. Schmidt, and M. Bachmann (World Scientific, Singapore, 2001).

[98] G. R. Golner and E. K. Riedel, Phys. Lett. **58A**, 11 (1976); K. E. Newman and E. K. Riedel, Phys. Rev. B **30**, 6615 (1984).

[99] A. Pelissetto and E. Vicari, Nucl. Phys. B **575**, 579 (2000).

[100] P. Butera and M. Comi, Phys. Rev. B **58**, 11 552 (1998).

[101] A different resummation that tries to keep track of the nonanalyticities of the $\beta$ function gives [60] $g^* \approx 1.39$.

[102] J. F. Nicoll and P. C. Albright, Phys. Rev. B **31**, 4576 (1985).

[103] We normalize $u$ as in Ref. [114]. Our coupling $u$ differs from the coupling used in Refs. [31,32] by a factor of 4! and from the definition used in Refs. [69,70] by a factor of 2.

[104] L. Schäfer, Phys. Rev. E **50**, 3517 (1994).

[105] L. N. Lipatov, Zh. Eksp. Teor. Fiz. **72**, 411 (1977) [Sov. Phys. JETP **45**, 216 (1977)].

[106] E. Brézin, J. C. Le Guillou, and J. Zinn-Justin, Phys. Rev. D **15**, 1544 (1977).

[107] Z. Y. Chen and J. Noolandi, Macromolecules **25**, 4978 (1992).

[108] W. H. Stockmayer, J. Polym. Sci. **15**, 595 (1955); Makromol. Chem. **35**, 154 (1960).

[109] H. Yamakawa and G. Tanaka, J. Chem. Phys. **47**, 3991 (1967).

[110] C. Domb and A. J. Barret, Polymer **17**, 179 (1976).

[111] J. des Cloizeaux, J. Phys. (France) **42**, 635 (1981).

[112] J. F. Douglas and K. F. Freed, Macromolecules **17**, 2344 (1984); **18**, 201 (1985).

[113] A. D. Sokal, in *Monte Carlo and Molecular Dynamics Simulations in Polymer Science*, edited by K. Binder (Oxford University Press, Oxford, 1995).

[114] J. Zinn-Justin, *Quantum Field Theory and Critical Phenomena*, 3rd ed. with corrections (Clarendon, Oxford, 1997).